REPORT NO.162

June, 1963.

THE COLLEGE OF AERONAUTICS

CRANFIELD

Experimental Investigation on a Cropped Delta Wing with Edge Blowing

- by -

A.J. Alexander, M.Sc., Ph.D., A.F.R.Ae.S.

SUMMARY

Low speed wind tunnel tests have been made on a 70° cropped delta wing with edge blowing both in the plane of the wing and at a downward deflection angle of 30°. The tests include six-component force and moment measurements, the distribution of static pressure at four chordwise stations, and quantitative measurements of the flow in the leading edge vortex.

At a constant incidence, blowing increases the size and strength of the leading edge vortices and moves the vortex cores outwards and upwards. Blowing also tends to suppress the secondary separation due to the entrainment effect of the jet. Blowing from the streamwise tips and trailing edge was relatively ineffective and most of the tests were made with blowing from the swept leading edges only, with tips and trailing edge sealed.

The lift magnification due to blowing, $\frac{\Delta C_{LB}}{C_{\mu}}$, decreased with decreasing incidence and increasing C_{μ}, but for small C_{μ} and high incidence, values of almost three were reached with leading edge blowing in the plane of the wing. With a suitable blowing distribution the conical nature of the flow is not disturbed and these lift increases are obtained with only a small centre of pressure movement, making the scheme particularly attractive for tailless aircraft.

$\frac{\Delta C_{L_B}}{C_\mu}$ Tests made with the jet sheet swept relative to the leading edge show that $\frac{\Delta C_{L_B}}{C_\mu}$ is reduced somewhat, but even with the jet emerging at an angle of only 10° to the swept leading edge, values of about two were obtained at low C_μ and high incidence. Providing conical flow is maintained, $\frac{\Delta C_{L_B}}{C_\mu}$ will be a function of $\frac{\alpha}{K}$ only and will increase as $\frac{\alpha}{K}$ increases. Thus the use of leading edge blowing with full engine thrust on highly swept wings will increase cruise lift to drag ratios and reduce landing and take-off speeds and distances by a substantial margin.

CONTENTS

		Page
	Summary	
	List of symbols	
1.	Introduction	1
2.	Model and experimental method	2
3.	Discussion of results	4
4.	Conclusions	19
	Acknowledgements	21
5.	References	22
	Figures	

LIST OF SYMBOLS

α	geometric wing incidence
β	angle of sideslip
θ	jet sweep angle, see fig.7
ϕ	edge droop angle, see fig.7
b	wing span = 1.62 ft.
c_o	root chord = 3.33 ft.
$\bar{c}$	aerodynamic mean chord $= \dfrac{\int_{-b/2}^{+b/2} c^2 dy}{\int_{-b/2}^{+b/2} c\, dy} = 2.60$ ft.
p_o, q_o	mainstream static and dynamic pressures
p	static pressure
s	wing semi-span
x,y,z	body axes, see fig.8
y_o, z_o	spanwise position and height of vortex core
H	total head measured in leading edge vortex
K	cotangent of leading edge sweep angle
O	origin of body axes at 0.50 c_o
S	wing area = 3.60 sq.ft.
C_p	static pressure coefficient $= \dfrac{p-p_o}{q_o}$
C_μ	blowing momentum coefficient $= \dfrac{\text{total momentum ejected}}{q_o \cdot S}$
C_L	lift coefficient $= \dfrac{\text{lift}}{q_o \cdot S}$
ΔC_{L_B}	lift increment due to blowing
C_D	drag coefficient $= \dfrac{\text{drag}}{q_o \cdot S}$
C_C	cross-wind force coefficient $= \dfrac{\text{cross wind force}}{q_o \cdot S}$

C_ℓ rolling moment coefficient about x axis = $\frac{\text{rolling moment}}{q_o . S . b .}$

C_m pitching moment coefficient about y axis (0.50 Co) = $\frac{\text{pitching moment}}{q_o . S . \bar{c}}$

C_n yawing moment coefficient about z axis (0.50 Co) = $\frac{\text{yawing moment}}{q_o . S . b .}$

1. Introduction

Many attempts have been made in recent years to improve the low speed characteristics of aircraft. Conventional trailing edge flaps give useful increases in lift which can be supplemented by a boundary layer control system but trimming the resulting large pitching moments reduces the effectiveness somewhat. The problem is particularly severe on highly swept tailless aircraft where lift coefficients are low in general and the use of trailing edge controls makes trailing edge flaps ineffective.

The reduction of the lift curve slope with aspect ratio is predicted by various theories both for attached flow[1] and with leading edge separation[2,3] but it is clear from the theory and from experimental evidence that the existence of leading edge separation and the associated leading edge vortices contributes to the lift and reduces the adverse effect of decreasing aspect ratio.

Since the leading edge vortices, or tip vortices in the case of low aspect ratio unswept wings, play such an important part in determining the flow pattern, it is clearly desirable to control their development in order further to increase their favourable influence. A promising method of control is to emit from the appropriate edges a jet in the form of a thin sheet. This jet (vortex) sheet rolls up in a manner similar to the rolling-up of the free vortex sheets and increases the strength of the resultant vortex, thus increasing the non-linear lift.*

Tests using this device have been made on a low aspect ratio straight wing[4], a 40° swept wing[5], both with tip blowing, and with leading edge blowing from a 70° delta wing[6]. In all these tests, edge blowing in the plane of the wing resulted in increased lift at constant incidence. The effect of blowing on the unswept wing was to change the spanwise lift distribution from elliptic to approximately constant loading due to the ability of the jet sheet to support a pressure difference. In the case of the wings with swept leading edges, the size and strength of the leading edge vortices was increased giving increased non-linear lift. In[5] at least, the increase in lift was obtained with little change in the longitudinal static stability over the greater part of the usable C_L range.

---

* Blowing increases the strength of the leading edges vortices at a given incidence and hence the adverse pressure gradient along the vortex core. Thus the incidence at which vortex breakdown occurs will be less with edge blowing. See Para.3.7 for discussion.

Although blowing increased the lift at constant incidence in the above tests the lift magnification $\frac{\Delta C_{L_B}}{C_\mu}$ was small and the aim of the present tests was to extend and amplify the existing exploratory work and, if possible, to improve on the results. The possibility of using leading edge blowing to improve lift-to-drag ratios was also investigated, and the tests covered a range of incidences and blowing momentum coefficients appropriate both to cruise and take-off conditions. Cruise values of C_μ could be obtained, but only at low speeds, and the effect of Mach Number could not be ascertained from this series of tests.

2. Model and experimental method

The model is shown mounted in the wind tunnel in fig.1. It is a 70° swept delta wing with cropped tips, of chord equal to one third of the root chord, and has an aspect ratio of 0.73. The main body is a hollow gunmetal casting and detachable brass edges form a continuous blowing slot round the periphery (of constant width 0.040 in.) except for a small region near the apex. The model is of rhombic cross-section, the total edge angle on both leading edges and tips is 20°, the trailing edge angle is 15°. Pressure plotting stations were located at $0.33c_o$, $0.49c_o$, $0.63c_o$ and $0.87c_o$ from the apex, and each station consisted of two continuous tubes each spanning half of the wing. Thirty-six static pressure holes (0.020 in. dia.) were drilled at each station to enable the spanwise static pressure distribution to be accurately described.

The tests were made in the College of Aeronautics 8ft. x 6ft. low speed wind tunnel, with the model supported on a Warden type six-component balance. High pressure air was fed to the model at the balance virtual centre through the hollow support strut, and constraints were kept to a minimum by the use of a flexible circular ring-main feed, (fig.5). A rotary seal at the centre enabled the model to be yawed.

The rate of mass flow of air to the model m_j, was measured using sharp-edged orifice plates in the main feed pipe. There was, of course, no loss of air as with an air bearing system. The jet total head distribution was measured just outside the slot and its momentum calculated on the assumption of isentropic flow. With blowing confined to the swept part of the leading edge, the direct component of thrust could be measured on the balance and the jet momentum calculated.

Owing to the difficulty of measuring the total head distribution accurately and of making allowances for induced effects on the balance measurement of thrust, there is a possible $\pm$ 3% inaccuracy in the values of C_μ.

In order to taper and direct the jet, thin grooved perspex strips were inserted in the slot (fig.4). Some preliminary tests with directed blowing showed that in order to obtain a given direction of the jet sheet, it was necessary to break up the jet into a large number of small jets each capable of individual direction. The individual jets recombined very close to the slot into a homogeneous sheet. The perspex strips were 0.5in. wide and 0.040in. deep with 0.020in. wide grooves having 0.040in. spacing cut at the appropriate angle to the leading edge. By varying the depth of the saw cut it was possible to vary the momentum ejected and thus obtain an approximately linear increase in momentum from the apex to the leading edge-wing tip junction (fig.8).

In this series of tests, all forces are referred to wind axes and moments to body axes (fig.9). Pitching and yawing moments are referred to a point on the model centre line at one half root chord.

In tests with blowing, the high pressure air caused the flexible ring main, (fig.5), to distort slightly and this induced additional forces and moments. To correct for these changes the model was removed periodically and a calibrator (fig.2) was attached to the balance strut. The calibrator consisted of a short length of pipe feeding air to the adjustable gap between two flanges. The gap was set such that with any given model configuration the rate of mass flow was the same for a fixed control pressure. Since the air was emitted radially from the virtual centre of the balance, the only forces and moments present should be those due to the distortion of the ring main. In order to allow for the slight inaccuracies in manufacture, the balance measurements were taken with the calibrator in a fixed position and then rotated through 180°. The average of the two sets of readings was taken to be the balance constraint correction due to blowing. Typical corrections, for a control pressure of 15 p.s.i. gauge at the orifice plates (C_μ = 0.178) with blowing from all edges are given below, coefficients based on V_∞ = 100 ft/sec.

Lift	-0.31 lbs.	C_L	-.007
Drag	-0.06 lbs.	C_D	-.001
Cross-wind force	+0.33 lbs.	C_C	+.008
Rolling moment	+1.17 lbs.	C_ℓ	+.017
Pitching moment	+0.22 lbs.	C_m	+.002
Yawing moment	+1.17 lbs.	C_n	+.017

The moments given here are referred to the balance virtual centre and wind axes.

Wind tunnel constraint corrections have not been applied to the present results since no suitable corrections are available, but conventional corrections are small, $\Delta\alpha = 0.5^\circ$ for $\alpha = 25^\circ$ and $\Delta C_D = 0.009$ for $C_D = 0.45$. Corrections have been applied to C_D, C_m, C_n, to allow for the drag of the incidence wire and the small exposed part of the main feed pipe.

In order to explore the vortex in detail, a five tube pitch-yawmeter (fig.3) was used which enabled traverses to be made in a spanwise plane. The head was similar to the five tube probe described in ref.7. The apex angle was 70° and the outside diameter 0.125in.

3. Discussion of results

As a preliminary to the main wind tunnel programme, a short series of tests was made, both with and without blowing at all edges, in order to provide some basic information on both the rig and the effects of blowing.

Wind speed was varied between 50 ft/sec and 200 ft/sec with no appreciable Reynolds number effect, hence tests without blowing were made at 200 ft/sec. to obtain the greatest accuracy but tests with blowing were made at lower wind speeds in order to achieve a reasonable range of C_μ. A few tests were made at a wind speed of 50 ft/sec. giving a maximum C_μ value of 1.55 but balance readings were less accurate at this low speed and most of the tests with blowing were made at 100 ft/sec. when the maximum value of C_μ was 0.39.

Comparative tests were also made without blowing (a) with the slot open and (b) sealed to prevent any airflow through the slot. In general, sealing the slot had little effect on the balance readings and the only appreciable changes were observed at the highest incidence on the rolling and yawing moments.

3.1. Lift

The jet sheet, originating at the leading edges and tips with blowing, rolls up to form the leading edge vortices in a manner similar to the rolling up of the free vortex sheets without blowing, although the pressure boundary condition is changed since the jet sheet can now support a pressure difference. This rolling up of the jet sheet has occurred in all the reported tests using slot blowing from streamwise tips and is a stable type of flow. A sharp change in lift and pitching moment occurs, however, in passing through zero incidence when the vortex moves from one surface to the other. Without blowing, of course, the flow is attached at zero incidence even with sharp leading edges, but with blowing the flow is apparently stable only when the jet sheet has rolled up, causing an abrupt change when the wing passes through zero incidence. The effect can be seen in fig.10 where the lift curve shows a discontinuity near $\alpha = 0$.

In the present tests near zero incidence with blowing it was possible to find an incidence at which the jet sheets oscillated from one surface to the other, producing a sinusoidal lift. The frequency of the oscillation was about one cycle per second at 100 ft/sec. and is thought to be associated with downwash lag in the following manner. Since the downwash angle $\epsilon_1 \sim \frac{C_L}{A}$, and with blowing C_L does not tend to zero as α tends to zero, it is possible to find an incidence α_1, which is less than the downwash angle for a given amount of blowing ($\alpha_1 < \epsilon_1$). If the wing is at positive incidence α_1 and the blowing is turned on, the jet sheet will tend to roll up over the top surface. As soon as the flow is established the average induced downwash will be greater than the incidence and the wing effectively at negative incidence so the sheet will move to the other surface. Thus an oscillatory motion is set up which would be undesirable in an aircraft, although it seems unlikely that this condition would be approached in practice.

Lift-incidence curves without blowing are shown in fig.11. At low incidence the camber effect of the edge droop (fig.6) increases the lift, but at higher incidence, with leading edge separations, the effect is small. The non-linear

curves are typical of sharp-edged, highly-swept wings, although near zero incidence the curve is close to the R.T. Jones lift curve slope for an aspect ratio 0.73 wing with attached flow. Sideslip angles of up to $\pm 5^{\circ}$ had no effect on lift. That sideslip has no appreciable effect on lift is fortuitous considering the non-linear nature of the problem. The changes in lift on the two halves of the wing are of opposite sign and, while not affecting overall lift, give large rolling moments (see Para.3.5).

The lift increment with blowing from all edges is plotted against momentum coefficient in figs. 12 ($\phi = 0$) and 13 ($\phi = 30^{\circ}$). At $\phi = 0$ for small values of C_μ and constant α the lift increased quite quickly, but above a C_μ of about 0.2 the rate of increase of lift was reduced. For a given value of C_μ the lift increment increased with incidence. The way in which lift changes with blowing and incidence can be explained in terms of the movement of the leading edge vortices. Application of edge blowing moves the leading edge vortices upward and outward particularly at small incidence (figs. 45, 46). The outward movement is accomplished in two stages. Firstly, the entrainment effect of the jet reduces and finally eliminates the secondary separation, causing the main vortex to move towards the edge. Secondly, at higher blowing pressures, the jet sheet will penetrate further into the mainstream before rolling up, and thus move the vortex core outboard again. At a sufficiently large value of C_μ the vortex core will move off the wing. This upward and outward movement of the vortex core with increasing C_μ means that the effect of the strong LE vortex is reduced somewhat since its height is greater than without blowing, particularly at small incidence, and the outward movement reduces the area of wing over which these low pressures are felt; hence the rate of increase of lift decreases with increasing C_μ at constant α. Again as incidence, or more strictly $\frac{\alpha}{K}$, increases the vortex core moves inboard without blowing so that the C_μ at which $\frac{\Delta C_{L_B}}{C_\mu}$ begins to level off is increased. Thus the condition for maximum relative benefit ($\frac{\Delta C_{L_B}}{C_\mu}$) will be small C_μ to limit the spanwise movement of the vortex and large $\frac{\alpha}{K}$ so that change in vortex height due to blowing is small.

With $\phi = 30^\circ$, Fig 13 shows that with leading edge droop the effect of incidence is roughly the same. The lift values include the direct jet lift ($C_\mu \sin\phi\cos\alpha$) this being approximately the difference between the $\phi = 0$ and $\phi = 30^\circ$ results at the larger values of C_μ.

Pressure plotting results (Para.3.7) with blowing from all edges showed that the majority of the lift increment due to blowing came from the forward swept part of the wing and that tip and trailing edge blowing was relatively ineffective. All further tests were then confined to leading edge blowing only with the undrooped ($\phi = 0$) edges. Simple theoretical considerations showed that in order to maintain conical flow with blowing it was necessary to increase the momentum ejected linearly along the swept edge from a zero value at the apex. This was achieved using the grooved perspex strips (fig.4). With these strips it was also possible to test the effect of sweeping the jet sheet relative to the edge (see Para.2). Fig.14 shows the lift increment due to blowing with tapered leading edge blowing only, the jet emerging normal to the leading edge ($\phi = 0$). Comparison with Fig.12 shows that the lift increment at a given value of C_μ is increased, particularly at small C_μ values. At large C_μ values ($C_\mu \sim 0.5$), the gains are small since in both cases C_μ is based on the total momentum ejected and the vortex movement (and hence lift increment) depends on the local C_μ value which is larger for leading edge blowing only (i.e. not blowing from tips and trailing edge) for a given overall C_μ.

In an attempt to analyse the results obtained with $\theta = 0^\circ$, the results of fig.14 were plotted in non-dimensional form in fig.14a, giving an approximately linear relation between $\frac{\Delta C_{L_B}}{K^2}$ and $\frac{C_\mu^{\frac{1}{2}}}{K}$ for fixed $\frac{\alpha}{K}$. Fig. 14b shows that a relation of the form $\frac{\Delta C_{L_B}}{K^2} \Big/ \frac{C_\mu^{\frac{1}{2}}}{K} = 0.20 + 1.24\left(\frac{\alpha}{K}\right)^{\frac{1}{2}}$ could exist.

Thus $\Delta C_{L_B} = 0.20\, C_\mu^{\frac{1}{2}} K + 1.24(\alpha . C_\mu . K)^{\frac{1}{2}}$. Adding this to Mangler and Smith's relation for the lift we have:

$$C_L = (2\pi\alpha + 0.20 C_\mu^{\frac{1}{2}})K + 1.24(\alpha . C_\mu . K)^{\frac{1}{2}} + 4\alpha^2$$

This relation is unsatisfactory in that the effects of blowing diminish with aspect ratio while the effects of the normal secondary separation do not. Using a relation of the form:

$$\frac{\Delta C_{L_B}}{K^2} \Big/ \frac{C_\mu^{\frac{1}{2}}}{K} = 0.20 + 1.37\left(\frac{\alpha}{K}\right)^{\frac{2}{3}} \qquad \text{(fig.14b)}$$

and the Brown and Michael expression for the lift we have:

$$C_L = (2\pi\alpha + 0.20\, C_\mu^{\frac{1}{2}})K + (5.0\alpha + 1.37\, C_\mu^{\frac{1}{2}})\, \alpha^{\frac{2}{3}}\, k^{\frac{1}{3}}$$

Here, at least, the effects of blowing and the unblown non-linear effects are comparable. A more exact relation must await the results of a theoretical investigation now in progress.

Figs. 15-20 show the effect of sweeping the jet sheet, for small C_μ values, $\theta = 0^\circ, 20^\circ, 50^\circ, 60^\circ, 70^\circ, 80^\circ$. The increase in lift with C_μ tends to be linear up to C_μ's of at least 0.03 for $\alpha > 0$. The beneficial effect of increasing α (or $\frac{\alpha}{K}$) is clearly visible. Apart from $\theta = 60^\circ$, where the blowing distribution was poor, the effect of increasing θ is fairly small up to $\theta = 70^\circ$. At $\theta = 80^\circ$, however, with full leading edge blowing (fig.20) there is a marked fall-off in lift at a given C_μ. This effect was investigated and attributed to the jet sheet clinging to the leading edge by means of the Coanda effect instead of emerging at the angle of the grooves as was the case up to $\theta = 70^\circ$. This effect delayed the rolling-up of the jet sheets and hence reduced the strength of the leading edge vortices.

In order to mitigate this effect, a further set of tests was made with $\theta = 80^\circ$ but with blowing from the first 6.5 in. of the leading edge slot only. (From 3 in. to 9.5 in. from the apex). The C_μ range was very much reduced owing to the smaller slot area (smaller mass flow) but fig.21 shows a considerable improvement over fig.20 for the higher incidence.

The lift augmentation ratio, $\frac{\Delta C_{L_B}}{C_\mu}$, is plotted against jet sweep angle θ in fig.22 for a C_μ value of 0.01, corresponding approximately to the cruise value. This shows clearly that the effect of increasing θ is small up to 70° but is large at greater angles when the jet sheet clings initially to the leading edge. The "starred" values of $\theta = 80^\circ$ were obtained with blowing close to the apex.

3.2 Drag

Drag is plotted against lift in fig.23 for $\phi = 0^\circ$ and 30° and C_μ values of 0 and 0.178, blowing from all edges. Blowing increases the drag at small incidence due to a small forward component of thrust, but drag is less with blowing at higher values of lift due to a reduction in the lift-dependent drag. The effect on drag of sealing the slot in the unblown case, and of sideslip between $\pm 5^\circ$ both with and without blowing, was negligible.

With blowing, at constant incidence, the drag will consist of four parts:

$$C_{D_{blowing}} = C_{D\ no\ blow} - C_\mu \cos(110 - \theta)\cos\alpha + \Delta C_{L_B} \tan\alpha + \Delta C_D$$

The first term is the drag without blowing, the second is the direct thrust component due to leading edge blowing, the third is the increment of induced drag due to the increased lift, and the last term is a small thrust due to the fact that most of the increased lift due to blowing acts on the forward part of the wing causing increased suctions on the forward facing surfaces. The first term can be obtained from fig.23 and the second and third terms are easily calculated, so it is of interest to plot the remaining term. It is, effectively, a reduction in induced drag and can be conveniently plotted in the form $-\frac{\Delta C_D}{C_L}$ vs ΔC_{L_B}.

Values for $\alpha = 5^\circ$, 10°, 15°, 20° with $\phi = 0^\circ$, 20°, 50°, 60°, 70°, 80° are plotted in figs. 24-27. The values of $-\Delta C_D$ are small and there is a good deal of scatter in the results. In general there is a tendency for $-\frac{\Delta C_D}{C_L}$ to increase with increasing θ

but the results for $\theta = 80^{\circ}$ are probably less reliable than the others.

The important fact is that the values of ΔC_D are always negative i.e. with leading edge blowing there is a small increment of thrust over and above the direct jet thrust measured wind off. With an aircraft designed to utilise its full thrust as leading edge blowing, this would bring a further increase in L/D, quite apart from obvious gains due to lower induced drag at a given lift coefficient.

3.3. Cross-wind force

Cross-wind force is plotted against the sideslip angle, β, in figs. 28 and 29. For the range of sideslip tested ($\beta = -5^{\circ}, 0^{\circ} +5^{\circ}$) the variation is apparently linear, although no tests were made at intermediate points. The results of ref.8 suggest that the variation will be linear between $\beta = \pm 5^{\circ}$ for the incidence range tested. For $\phi = 0^{\circ}$ the blowing results differ only slightly from the unblown results, due to asymmetries in the blowing giving a small force at zero sideslip. Similar observations may be made for $\phi = 30^{\circ}$. It is concluded that the effect of symmetrical edge jets on cross-wind force is small.

3.4. Pitching moments

Pitching moments about half root chord are plotted against lift in figs. 30 - 32. Again, sealing the slot without blowing and sideslipping up to 5° had very little effect. Without blowing, $\phi = 0^{\circ}$, the pitching moment varied linearly with lift.

The effect of blowing from all edges and of drooping the edges can be seen in fig.30. With $\phi = 0^{\circ}$, the effect of blowing on pitching moments was small at high incidence but larger at small incidence. There was also a discontinuity near $\alpha = 0$ due to the vortex moving from one surface to the other corresponding to the discontinuity in lift (see Para.31). Drooping the edges 30° moved both the aerodynamic centre and centre of pressure to the rear, almost $0.1\,c_o$. Blowing with $\phi = 30^{\circ}$ aggravated this effect and introduced considerable non-linearities, although these are probably due mainly to non-uniform blowing.

Fig. 31 shows the effect of increasing C_μ for the case $\theta = \phi = 0$ with leading edge blowing only. In this case the effect of blowing is to move the aerodynamic centre and centre of pressure forward as the major effect of the blowing is felt on the forward part of the wing*. Fig.32 shows changes due to increasing θ with $\phi = 0^\circ$ and $C_\mu = .014$. Here the tendency is for the centre of pressure to move back with increasing θ since sweeping the jet delays the rolling up of the sheet somewhat.

3.5. Rolling moments

In figs. 33 and 34 the rolling moment about the model centre line is plotted against sideslip angle β, and the corresponding ℓ_v values ($\equiv \frac{\partial C_\ell}{\partial \beta}$) are plotted against lift in fig.35. The variation of C_ℓ appears to be linear within the range $-5^\circ \leqslant \beta \leqslant +5^\circ$ and evidence from ref.8 supports this.

The rolling moments induced on a delta wing in sideslip are due mainly to an asymmetric pattern of the leading edge vortices (fig.41). The vortex on the advancing edge remains tightly rolled but that on the retreating edge becomes more diffuse and weaker. Thus for negative sideslip there is a positive rolling moment which increases with increasing incidence. The results for $\phi = C_\mu = 0$ are shown in fig.33; only at the highest incidence was there an appreciable change due to sealing the slot.

Without blowing, the rolling moment due to sideslip is caused mainly by a weakening of one leading edge vortex relative to the other. With blowing, however, the rolling up of the leading edge vortex sheets is partly controlled by the edge jets, which are comparatively unaffected by sideslip, and should resist this deformation of the flow pattern. This should tend to reduce the magnitude of C_ℓ, and hence ℓ_v, at a given lift. From the results for $\phi = 0$, however, it appears that this is only true at incidences above 15° ($C_L > 0.5$).

---

* At C_μ values corresponding to the landing case (≈ 0.4), the forward movement of the aerodynamic centre is 2-3% of the root chord and stability considerations may limit the usable C_μ under these conditions.

The effect of drooping the edges, $\phi = 30^{\circ}$, (fig.35) is to reduce ϵ_v at a given lift. Without blowing, at least part of the reduction is due to the decrease in span due to the drooped edge and with blowing, the further reduction is the result of the direct jet reaction producing lift but no extra rolling moment.

3.6. Yawing moments

Yawing moments about half mean chord are plotted against sideslip angle β for $\phi = 0^{\circ}$ and 30° in figs. 36 and 37. Again the variation was linear in the range of sideslip tested. Corresponding values of n_v are plotted against lift in fig.38.

The asymmetric pressure distribution due to sideslip, (see Para.3.5), will produce a yawing moment on a wing with thickness due to the pressure differential on the side area. As with the rolling moments, sealing the slot has an appreciable effect at the highest incidence. For $\phi = 0^{\circ}$, the effect of blowing from all edges is small.

Drooping the edges 30° increases the side area by equal amounts fore and aft of the half chord position, but since the chordwise loading is concentrated towards the apex the effect of edge droop is to increase the magnitude of the yawing moments compared with the $\phi = 0^{\circ}$ case. There is a change in $C_{n_\beta} = 0$ due to asymmetric blowing but n_v is scarcely affected. There is a reduction in n_v at a given lift with blowing due to the direct jet lift (see Para.3.5).

3.7. Pressure measurements and flow visualisation

The spanwise variation of static pressure was measured at four chordwise stations, $0.33c_o$, $0.49c_o$, $0.63c_o$ and $0.87c_o$. Without blowing, the range of incidence was $\alpha = 2^{\circ}$, 5°, 10°, 15°, 20°, 25° and with blowing, $\alpha = 5^{\circ}$, 10°, 15°. The results are shown in figs. 39-43. The pressures measured on the starboard wing are on the left hand side of the figures, i.e. the wing is viewed from the stream direction.

Without blowing (figs. 39-41) the pressure distributions are typical of wings with sharp, highly swept leading edges. The suction peak which occurs beneath the vortex core can be clearly seen, particularly at the more forward stations, and small suction peaks are evident at angles of incidence as low as two degrees (fig.39). The slight bluntness of the leading edge, due to the slot, does not appear to prevent the flow separating without blowing, even at very low incidence. At higher incidence, the extent of the secondary separation is indicated by a region of roughly constant pressure outboard of the main vortex core. Reasonable agreement is obtained with the results of ref.9, in which surface static pressures were measured on a 70° true delta wing.

Fig.40 shows the chordwise variation of static pressure, without blowing, at constant incidence, $\alpha = 35^{\circ}$. The flow remains approximately conical in form back to as least $0.65c_o$, i.e. to the leading edge-tip junction. At $0.87c_o$, however, there has clearly been a considerable reduction in lift due to the effect of the trailing edge. It is not thought that vortex breakdown is occurring at this incidence at the rear station. Ref.10 shows that vortex breakdown occurs behind the trailing edge of a 70° swept plate at $\alpha = 25^{\circ}$, although the effect of cropping a delta wing has not been investigated. The suction peak rises steadily with incidence at $\frac{x}{c_o} = 0.87$ and does not show the reversal of this trend at high incidence which indicates vortex breakdown in ref.10. Fig.41 shows the effect on the pressure distribution of five degrees of sideslip. The basic flow pattern appears to be unchanged, but the vortex on the advancing edge is stronger and has moved slightly inboard, while the vortex on the retreating edge is weaker but does not appear to have moved. These results are generally in agreement with ref.11; at higher angles of sideslip the vortex on the retreating edge moves towards the leading edge and the secondary separation is no longer visible.

The increase in vortex strength due to edge blowing can be seen in fig.42. In order to maintain conical flow with blowing, the momentum ejected should increase linearly from a zero value at the apex and this is almost achieved using the grooved perspex strips ($C_\mu = 0.096, \beta = 0^{\circ}$). With an open slot, blowing from all edges, the momentum distribution was more nearly constant i.e. too much air was ejected near the apex, and resulted in a very non-uniform chordwise pressure

distribution. Even with blowing, the load at the rearmost pressure plotting station, $0.87c_o$, was still small (see Para.3.1). With blowing from the leading edges only there will be a sudden reduction in the strength of the leading edge vortex sheet at the leading edge wing tip junction. This would tend to reduce the incidence at which vortex breakdown occurs but it is not thought to have occurred in the present tests. Further information is desirable, however, and a more detailed investigation into the effects of blowing on vortex breakdown is to be made shortly.

Fig.43 compares the results obtained with and without leading edge blowing only with the theories of Brown and Michael[2] and Mangler and Smith[3]. The similarity between the pressure distributions for the experimental results with blowing and the theoretical values without blowing is to some extent fortuitous and is dependent on the value of C_μ, but it is interesting to note that the existence of the secondary separation is mainly responsible for the discrepancy between theory and experiment for the spanwise position of the vortex[12]. The separation which occurs without blowing is suppressed gradually by the entrainment effect of the edge jet and can be entirely suppressed with quite small values of C_μ (about 0.05 at $\alpha = 20^\circ$)(see also ref.12).

The movement of the vortex core with incidence ($C_\mu = 0$) is shown in fig.44 and the present results are compared with other experimental values[9,13] and with the theories of Brown and Michael[2] and Mangler and Smith[3]. The positions were estimated using a tuft grid and using the five-tube pitch-yawmeter. The experimental results are in reasonable agreement except for the spanwise positions of the vortex given by ref.13 which appear to be in error. The theory of Brown and Michael predicts the height of the vortex core reasonably well but both theories,[2,3], are seriously in error with regard to the spanwise position. Some reasons for the discrepancy are discussed in ref.12. The effect of leading edge blowing only is shown in figures 45 and 46 where the results with blowing, ($C_\mu \simeq 0.05$ and 0.1 $\theta = 0,50^\circ$) are compared with the mean values obtained without blowing. At zero incidence with blowing there is quite a powerful vortex, but without blowing there is no vortex on this symmetrical wing. Thus for a given C_μ the effect of blowing on the vortex position is greatest at low incidence and decreases at higher incidence where a

vortex would exist without blowing. A change in θ from 0° to 50° at constant C_μ does not change the vortex position greatly as would be expected from the lift results (fig.22). At much larger values of C_μ ($\theta = 0^\circ$, $C_\mu = 0.56$) the vortex core is well above the wing and at incidences below 15° is outboard of the leading edge.

A series of traverses in a spanwise plane were made with the five-tube pitch-yawmeter (fig.3) at one incidence, with and without blowing, to show the changes in flow pattern. The apparatus was also used to locate the position of the vortex core as a check on the tuft observations. Results for $\alpha = 10^\circ$, $C_\mu = 0$ and 0.048 are compared in figs. 47 and 48. Values of $\frac{H-p_o}{q_o}$ are plotted against non-dimensional semi-span $\frac{y}{s}$; this gives a good indication of the losses occurring and shows the structure well. The extent of the leading edge vortex is defined by the value 1.0 of the variable.

Without blowing (fig.47) the vortex core and the region of secondary separation can be clearly seen. The minimum value of $\frac{H-p_o}{q_o}$ recorded was -0.79, which indicates a high axial velocity although the actual value could not be calculated owing to the difficulty of measuring pressure in the core with the five-tube probe. With blowing, $C_\mu = 0.048$, (fig.48) a much larger region is affected. The height of the vortex core is increased and it is moved outboard. The secondary separation has been eliminated and it is possible to trace the effect of the jet for almost a full turn of the sheet. Minimum value of $\frac{H-p_o}{q_o}$ is now -2.5, indicating a considerable increase in velocity over the unblown case.

3.8. Some practical applications of leading edge blowing

While it is possible to tolerate, at relatively low speeds, an aircraft composed of a number of separate items (fuselage, wings, tail, engines etc.) at much higher speeds the case for a fully integrated aircraft is unanswerable. In the early stages, the application of a new idea is not easy to foresee and is usually fraught with engineering difficulties, e.g the jet flap, but it was felt worthwhile to include some thoughts on the possible uses of leading edge blowing if only as a basis for further discussion.

The use of leading edge blowing presupposes a very highly swept wing and the experimental results show that considerable gains in pressure lift are achieved without any direct thrust loss, at least at low speeds. Very little information on the effect of Mach number is available, although some unpublished work carried out at the College of Aeronautics with slot blowing from the shoulder of a half cone showed that even at a Mach number of 2.0, a much larger vortex was produced by the blowing and appreciable increases in lift obtained. Owing to the small scale of the experiment, however, it was not possible to measure the increase of lift accurately, although $\frac{\Delta' C_{L_B}}{C_\mu}$ was of the order of one at small C_μ values. Provided the wing and vortex sheet are well inside the mach cone, the effects of mach number will probably not be excessive at small α although since the pressure on the top surface cannot fall below absolute vacuum there is a definite limit to the increase in non-linear lift that can be achieved. Thus it seems likely that appreciable increases in lift will still be achieved even for Mach numbers around two and since lift to drag values are generally low on highly swept wings, even small improvements are well worthwhile.

In order to feed air to the leading edge the choice seems to lie between conventionally mounted jet engines (i.e. at the rear) with a large amount of ducting and its attendant losses and space problems, and engines mounted much closer to the leading edge with a fishtail nozzle forming the leading edge slot. The latter can be further sub-divided into a large number of small jet engines spaced at intervals down the leading edge or perhaps four large jets mounted in the fuselage at the nose (two per side) and exhausting near the wing apex. Propulsion would still be obtained from direct jet thrust and this would mean that the jet exhaust could not be inclined more than say 20° from the aircraft centre line in the plane of the wing except during landing. Owing to the tendency for the jet to cling to the leading edge when it is highly swept (see Para.3.1), it would be preferable to concentrate the blowing in the region of the wing apex. Thus from an aerodynamic viewpoint, fuselage mounted jets exhausting close to the wing apex are preferred.

Moving the engines from the vicinity of the trailing edge to the apex involves a major redistribution of the weight and, as a result, the passenger load would have to be moved aft. A tentative layout suggests that an appreciable part of the fuselage will project aft of the trailing edge instead of forward of the apex as with the present "Concord" aircraft. Jet exhausts emanating from the wing apex may cause some heating problems on the wing upper surface, but the fact that they will roll up into the leading edge vortex core and hence do not actually touch the wing, combined with the temperature drop in the vortex core caused by the rotating flow, suggests that the heating problem may not be severe. Pressure fluctuations on the wing surface under the vortex core would also increase somewhat. Nose mounted jets will undoubtedly increase the noise level inside the aircraft unless additional lagging is provided, but noise in the far field will probably be less owing to the shielding effect of the aircraft itself.

In order to get some idea of possible improvements in performance which would be obtained with leading edge blowing close to the apex, a simple comparison has been made between two aircraft of the same size and weight and roughly representative of the supersonic airliner.

The conventional aircraft considered has a gross weight of 300,000 lbs. and a maximum total thrust of 100,000 lbs. It is assumed to cruise at $\alpha = 4^{\circ}$ and have a lift/drag ratio of eight ($C_L = 0.1$, $C_D = 0.0125$). The unconventional aircraft is the same size but has its engines mounted in the nose, exhausting in the form of a sheet near the wing apex in the plane of the wing at an angle of 15° to the aircraft centre line.

For cruising, the assumption is made that $\frac{\Delta C_{L_B}}{C_\mu} = 1.0$ and hence for the same lift ($C_L = 0.1$) α is reduced with a consequent reduction in lift dependent drag. (It is further assumed that blowing does not increase the wave drag). It should be noted here that the lift increment due to blowing depends on the momentum ejected over the wing i.e. depends on the gross and not the net thrust. (A value of gross thrust = 1.5 x net thrust has been taken here). Under these conditions it can be shown that a thrust of only 90% of the thrust of the conventional aircraft is

sufficient to fly the aircraft at $\alpha = 3.3^{\circ}$ and the lift/drag ratio is increased to 8.97, an increase of 12%, even without a further allowance for the decrease in fuel and engine weight. More detailed calculations were not made owing to the uncertainty of the basic assumption $\frac{\Delta C_{L_B}}{C_\mu} = 1.0$, but this is probably not greatly in error and more detailed calculations with allowances for decreases in fuel and engine weight based on an accurate value for $\frac{\Delta C_{L_B}}{C_\mu}$ are expected to show increases in lift/drag ratios of the same order.

At take off, $\frac{\Delta C_{L_B}}{C_\mu}$ will be larger than for cruise, owing to the higher incidence, $\alpha = 15^{\circ}$. The plain wing is assumed to give a C_L of 0.5 at this incidence without blowing, rising to $C_L = 0.65$ with $C_\mu = 0.195$. Thus the take-off speed is reduced by about 12%. On landing (weight = 170,000 lbs.), C_L reaches 0.79 at $C_\mu = 0.417$ giving a reduction in landing speed of 20%, assuming that some form of swivelling nozzle will enable the engines to be run at full thrust, the net thrust being reduced to an appropriate value by deflecting the jets away from the aircraft.*

Thus it seems that the application of leading edge blowing to a supersonic airliner of conventional size and weight would show useful gains in cruise and take-off performance and very substantial gains in landing performance, which is in many cases the limiting factor in present day designs. No attempt should be made to minimise the difficulties involved in the use of leading edge blowing, especially on a large scale, but none would appear to be insuperable, especially when compared with the difficulties involved in conventional designs.

---

* Stability considerations may limit the usable C_μ on landing (see Para.3.4).

4. Conclusions

Low speed wind tunnel tests have been made on a 70° cropped delta wing to investigate the effects of edge blowing.

The main conclusions are as follows:

1. Edge blowing, in particular leading edge blowing, increases the lift by increasing the size and strength of the leading edge vortices at a given incidence. The increase in lift is due mainly to an increase in the non-linear contribution.

2. The edge jet sheets always roll up to form leading edge vortices giving steady flow patterns with the wing at incidence. At a sufficiently small incidence, however, the jet sheets oscillate from one surface to the other due to a downwash lag effect. This is unlikely to be a practical limitation since the incidences are of the order of 0.25°.

3. The effect of blowing from the streamwise tips and trailing edge was small, and best results were obtained with leading edge blowing only. The use of small grooved perspex strips enabled both the distribution and direction of the blowing to be controlled and except for very highly swept jets there was very little reduction in lift augmentation with increasing θ.

4. Maximum values of the lift augmentation, $\frac{\Delta C_{L_B}}{C_\mu}$, were obtained for small values of C_μ (<0.05) and large values of incidence. The maximum value achieved was 2.8 for $\alpha = 20^{\circ}$ and $\theta = 0^{\circ}$, 20° with blowing in the plane of the wing i.e. no direct jet lift.

5. There was no appreciable Reynolds number effect in the range 0.8×10^6 to 3.2×10^6.

6. Sideslip up to $\pm 5^{\circ}$ had no effect on lift, drag or pitching moment.

7. The effect of edge blowing in the plane of the wing on the lateral derivatives ℓ_v and n_v at a given lift was small. The effect on pitching moment depended on C_μ and θ, but for practical values of C_μ it was not excessive.

8. Due to the higher suction forces acting mainly on the forward facing surfaces, the values of thrust were slightly higher than would have been expected from consideration of the direct jet thrust component.

9. If leading edge blowing were used to reduce landing speeds using air bled from the jet engine compressors, a bleed of 10% of the mass flow would reduce landing speeds by about ten knots, i.e. roughly the reduction obtained by the use of blowing boundary layer control with trailing edge flaps on more conventional planforms. Ducting would be a problem because of the length involved (approx.200ft.) and the relatively large area (about 5% of wing cross sectional area).

10. If the total jet thrust were available in the form of leading edge slot blowing, preferably close to the apex, reductions in take-off and landing speeds of 12% and 20% respectively could be achieved, assuming that the direction of the jet could be suitably controlled. Although the effects of Mach number are not known accurately, increases in the lift/drag ratio of about 10% would appear feasible.

Acknowledgements

The work described in this report formed part of the Author's Ph.D. thesis.

The author is indebted to Professor G.M. Lilley for his advice and encouragement during the course of the work.

Thanks are also due to Mr. S.H. Lilley, Mr. D. Horn and Mr. I.McRae for their help with the wind tunnel programme, and to Miss R. Fuller who performed the lengthy computations.

5. References

1. Jones, R.T. — Properties of low aspect ratio pointed wings at speeds below and above the speed of sound. N.A.C.A. Report No. 835, 1946.

2. Brown, C.E. Michael, W.H. — Effect of leading-edge separation on the lift of a delta wing. J.Ae.S. Vol.21, 1954, p.690.

3. Mangler K.W. Smith J.H.B. — A theory of the flow past a slender delta wing with leading edge separation. Proc. Roy. Soc. A. Vol.251, 1959, pp.200-217.

4. Smith, V.J. Simpson, G.J. — A preliminary investigation of the effect of a thin high velocity tip jet on a low aspect ratio wing. Australian Dept. of Supply. Note ARL.A163. 1957.

5. Ayers, R.F. Wilde, M.R. — Unpublished College of Aeronautics Thesis.

6. Trebble, W.J.G. — Low speed wing tunnel experiments with blowing from the leading edge of a delta wing with 70° sweepback. Unpublished M.O.A. Report.

7. Bryer, D.W. Walshe, D.E. Garner, H.C. — Pressure probes selected for mean-flow measurements. Exploration of turbulent boundary layers. A.R.C. Report 17,997. November 1955.

8. Peckham, D.H. — Low speed wind tunnel tests on a series of uncambered slender pointed wings with sharp edges. A.R.C. R. and M. 3186, 1958.

9. Marsden, D.J.
Simpson, R.W.
Rainbird, W.J.
The flow over delta wings at low speeds with leading edge separation.
College of Aeronautics Report 114, 1957.

10. Lambourne, N.C.
Bryer, D.W.
The bursting of leading-edge vortices - some observations and discussion of the phenomenon.
A.R.C. R. and M. 3282, 1962.

11. Harvey, J.K.
Some measurements on a yawed slender delta wing with leading edge separation.
A.R.C. R. and M. 3160, 1958.

12. Alexander A.J.
Experiments on a delta wing using leading edge blowing to remove the secondary separations.
College of Aeronautics Report 161, 1963.

13. Lambourne, N.C.
Bryer, D.W.
Some measurements of the positions of the vortices for sharp edged delta and swept back wings.
A.R.C. Report 19,953. March 1958.

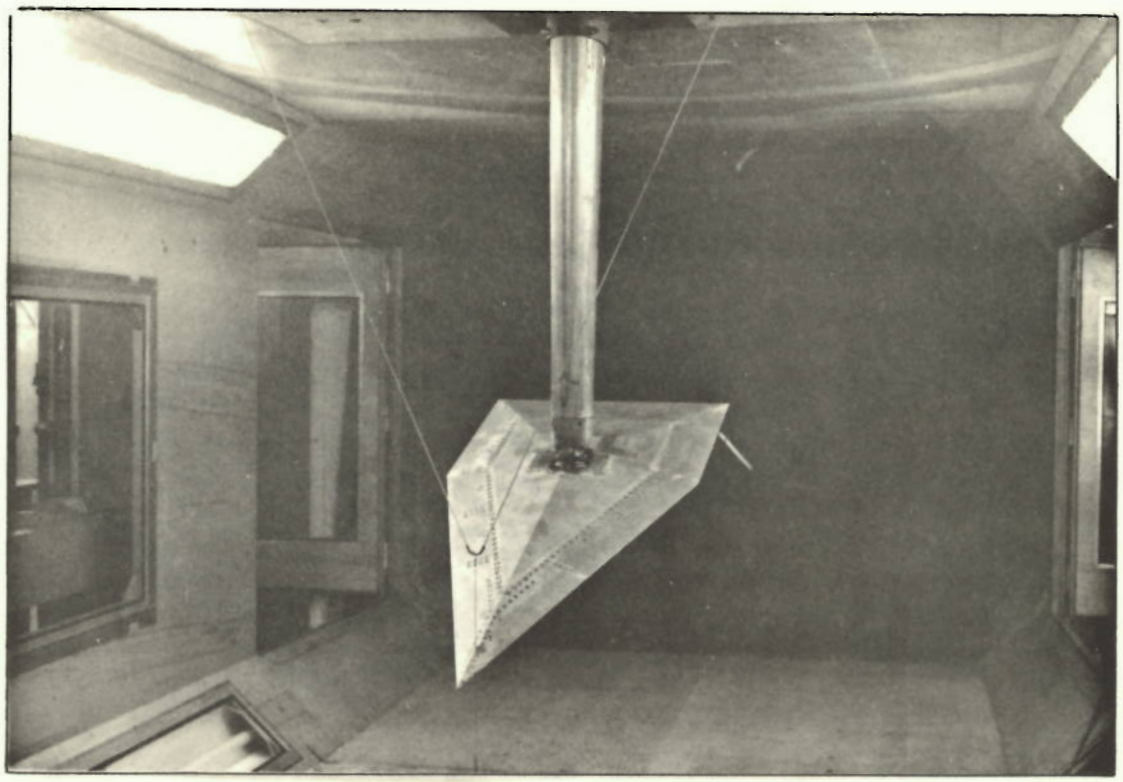

FIG. 1 MODEL MOUNTED IN WIND TUNNEL

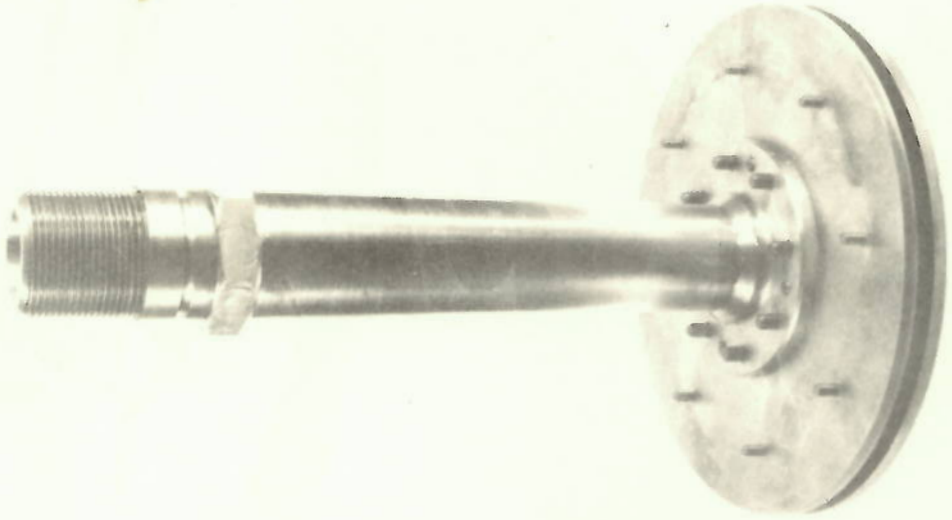

FIG. 2 THE CALIBRATOR

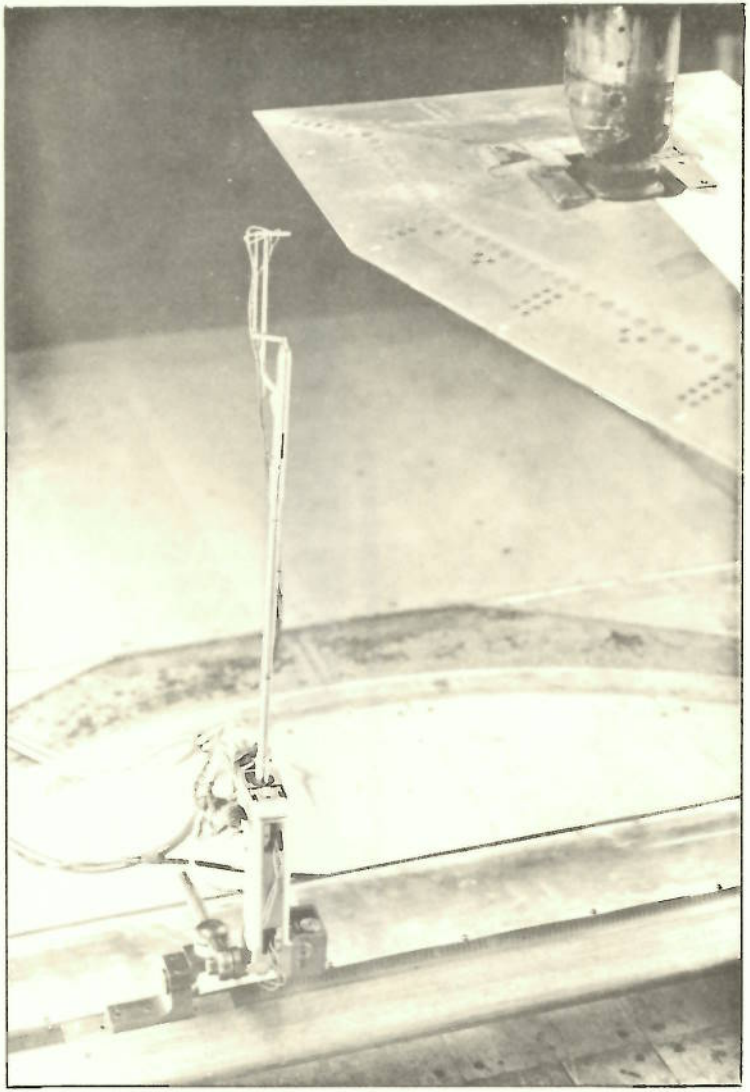

FIG. 3 FIVE TUBE PITCH-YAW METER

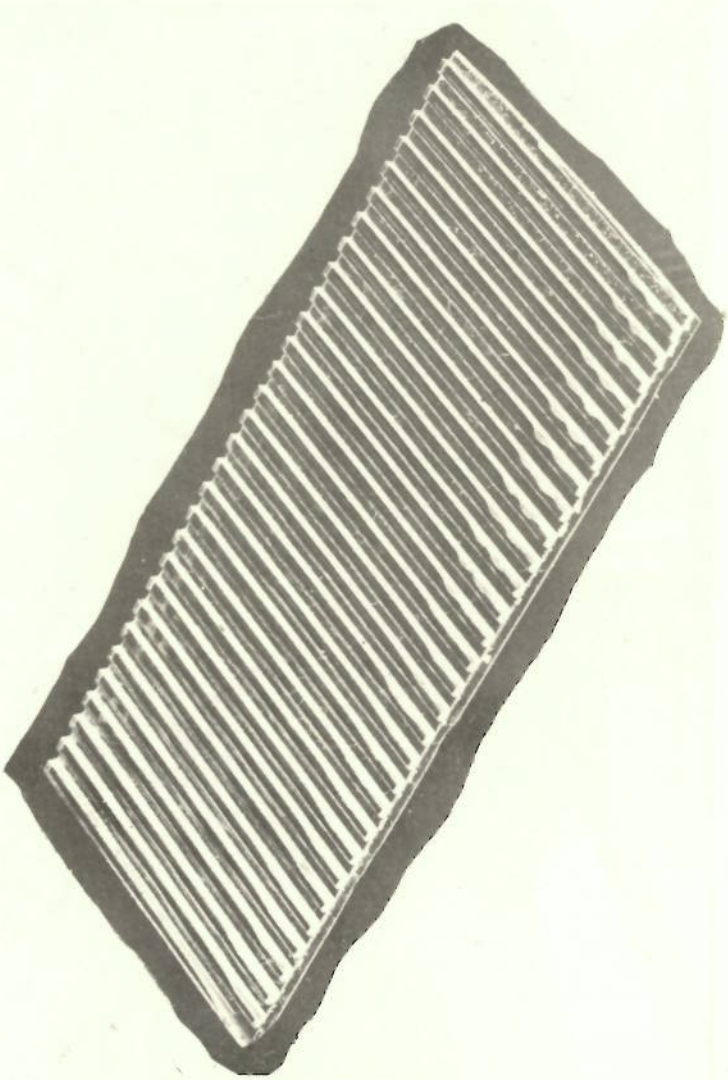

FIG. 4 PERSPEX EDGE STRIPS

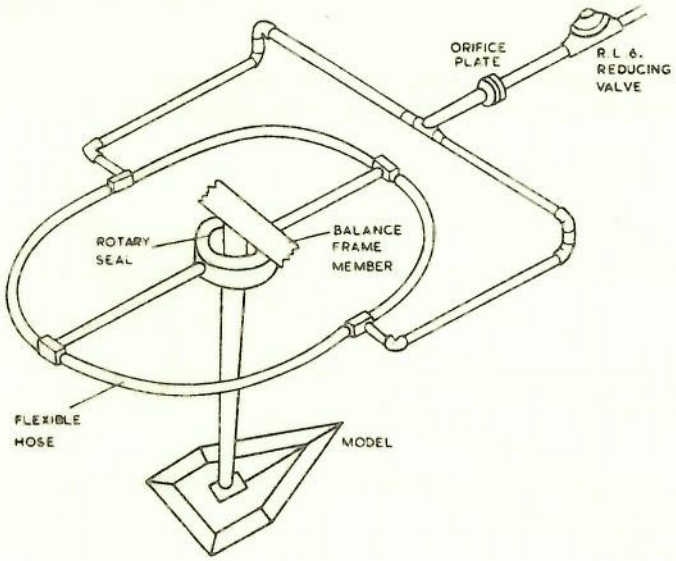

FIG.5. MODEL MOUNTING.

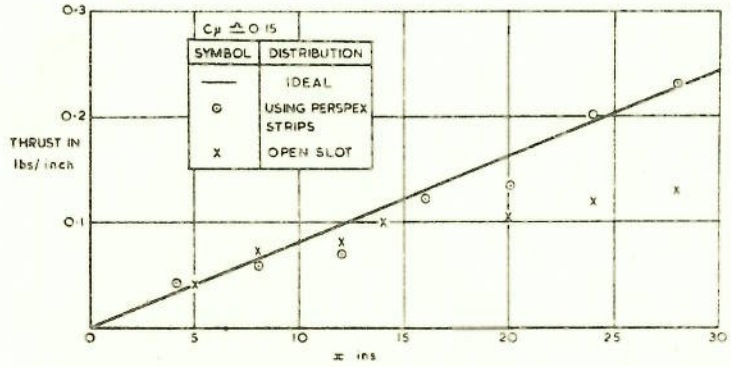

FIG.8. BLOWING MOMENTUM DISTRIBUTION ALONG LEADING EDGE.

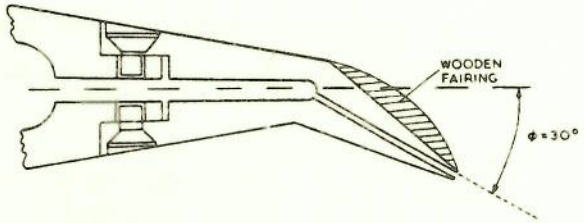

FIG. 6. 30° DROOPED EDGE.

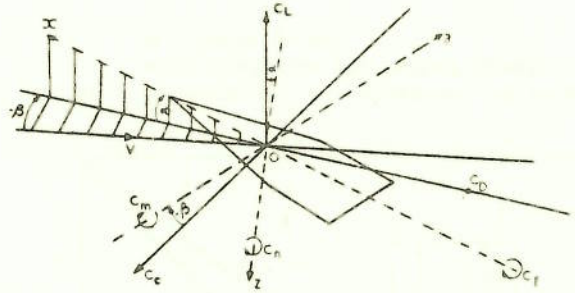

FIG.9. FORCE AND MOMENT AXES SYSTEM.

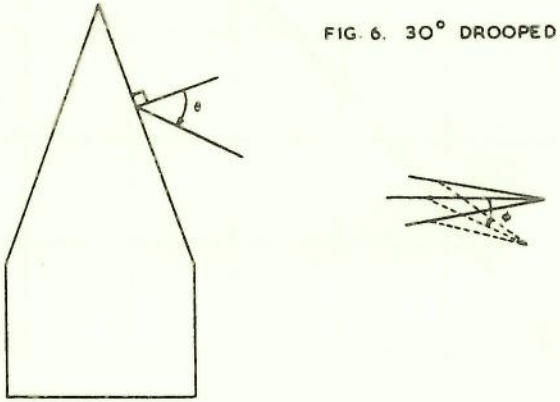

FIG. 7. DEFINITION OF θ & ϕ.

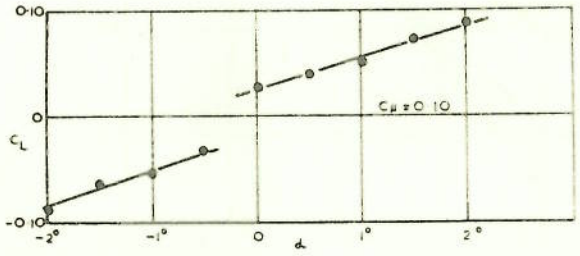

FIG.10. JET SHEET INSTABILITY NEAR ZERO INCIDENCE BLOWING FROM ALL EDGES.

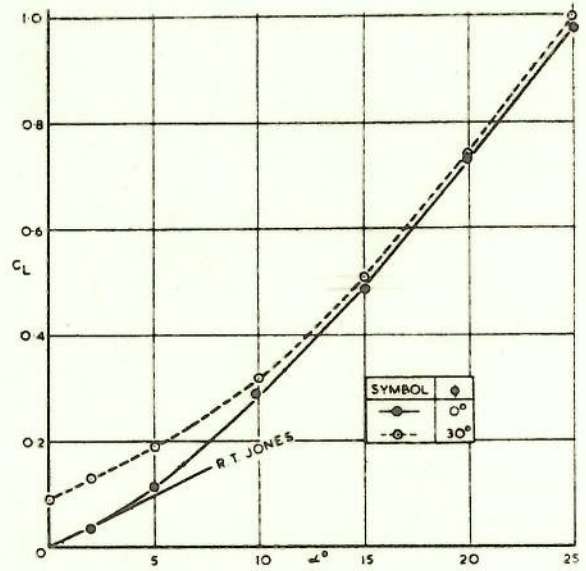

FIG.11. VARIATION OF LIFT WITH INCIDENCE. $C\mu = 0$.

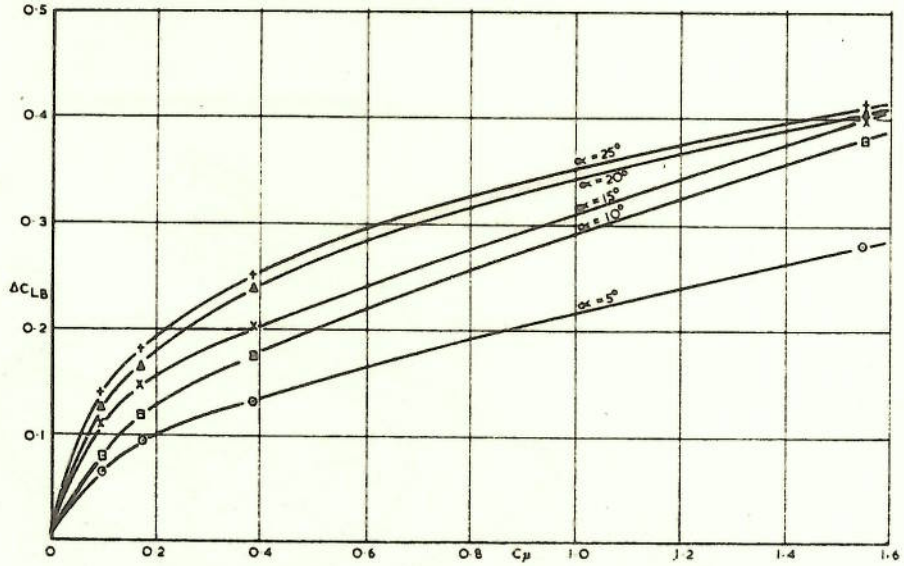

FIG. 12. VARIATION OF LIFT INCREMENT DUE TO BLOWING WITH MOMENTUM COEFFICIENT. BLOWING FROM ALL EDGES. $\phi = 0°$.

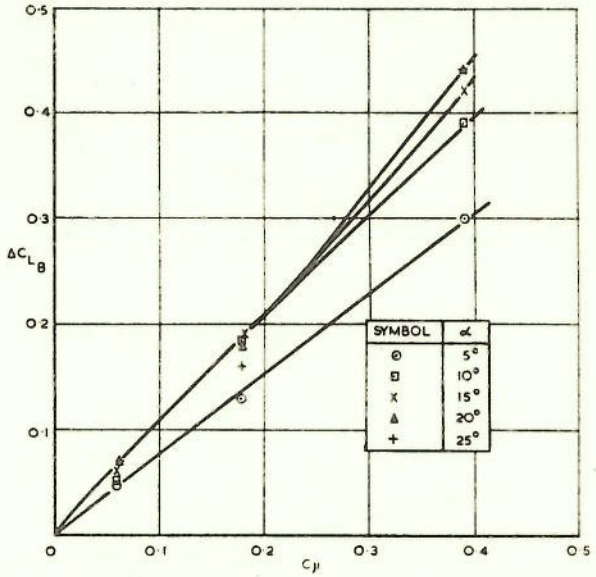

FIG.13. VARIATION OF LIFT INCREMENT DUE TO BLOWING WITH MOMENTUM COEFFICIENT BLOWING FROM ALL EDGES $\phi = 30°$.

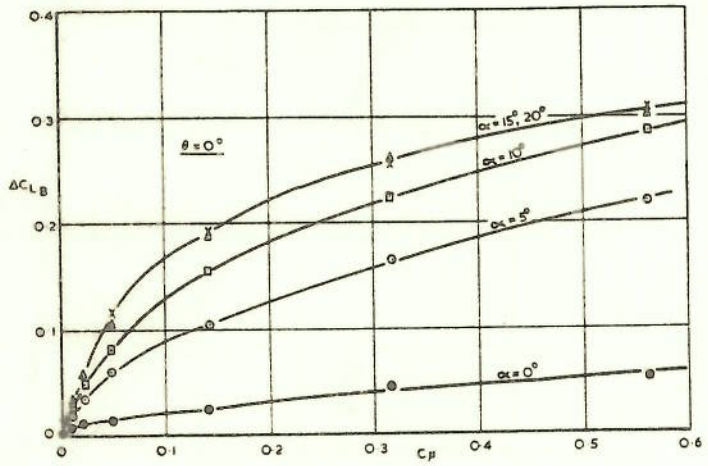

FIG. 14. VARIATION OF LIFT INCREMENT DUE TO BLOWING WITH MOMENTUM COEFFICIENT. L.E. BLOWING ONLY. $\phi = \theta = 0$.

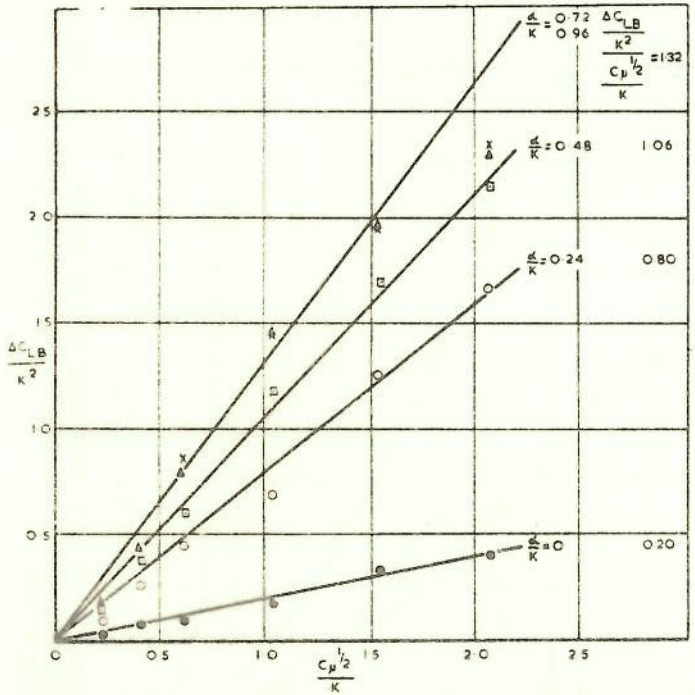

FIG. 14a. VARIATION OF $\frac{\Delta C_{LB}}{K^2}$ WITH $\frac{C\mu^{1/2}}{K}$ FOR $\phi = \theta = 0$.

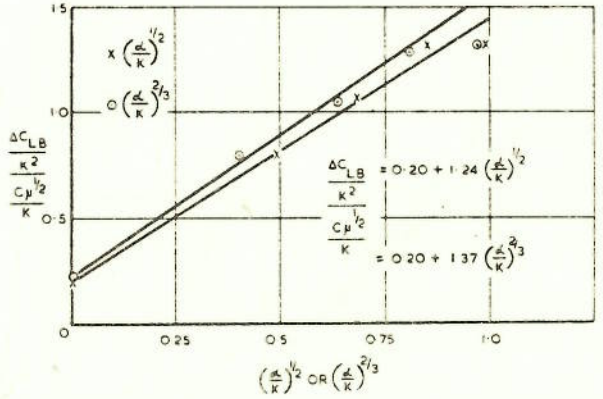

FIG. 14b. VARIATION OF $\frac{\frac{\Delta C_{LB}}{K^2}}{\frac{C\mu^{1/2}}{K}}$ WITH $\left(\frac{\alpha}{K}\right)^{1/2}$ OR $\left(\frac{\alpha}{K}\right)^{2/3}$.

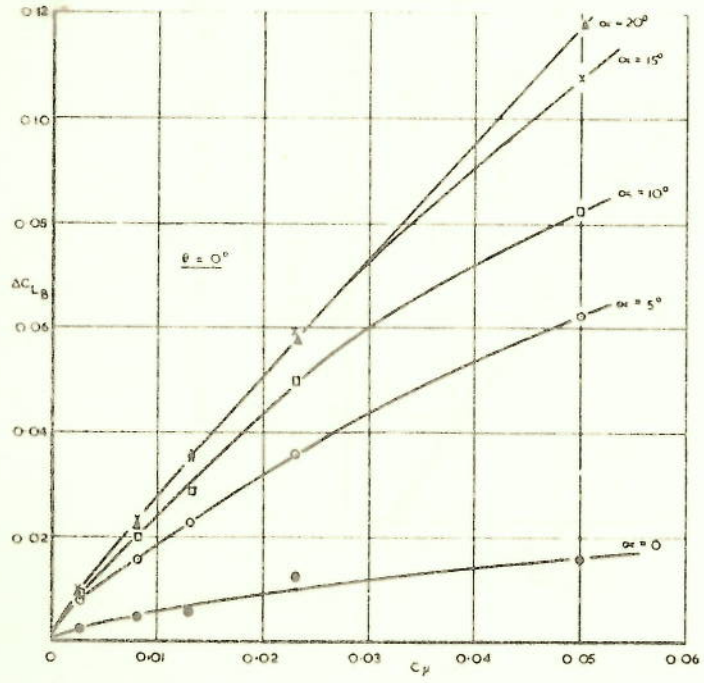

FIG. 15. VARIATION OF LIFT INCREMENT DUE TO BLOWING WITH MOMENTUM COEFFICIENT. L.E. BLOWING ONLY. $\phi = \theta = 0$.

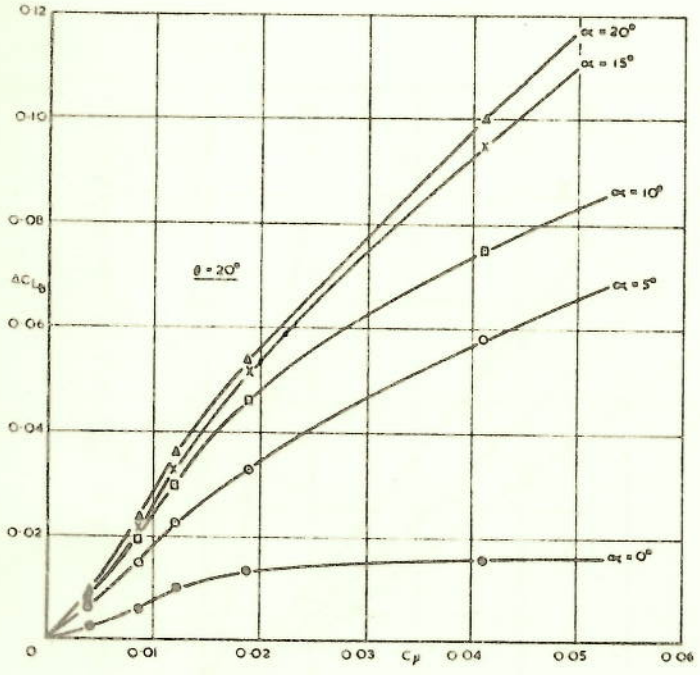

FIG. 16. VARIATION OF LIFT INCREMENT DUE TO BLOWING WITH MOMENTUM COEFFICIENT. L.E. BLOWING ONLY. $\phi = 0°$, $\theta = 20°$.

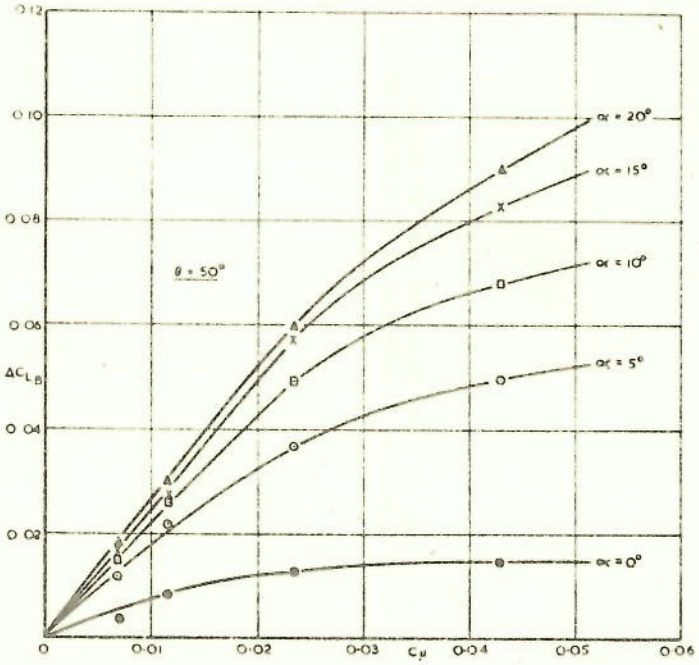

FIG. 17. VARIATION OF LIFT INCREMENT DUE TO BLOWING WITH MOMENTUM COEFFICIENT L.E. BLOWING ONLY. $\phi = 0°$, $\theta = 50°$.

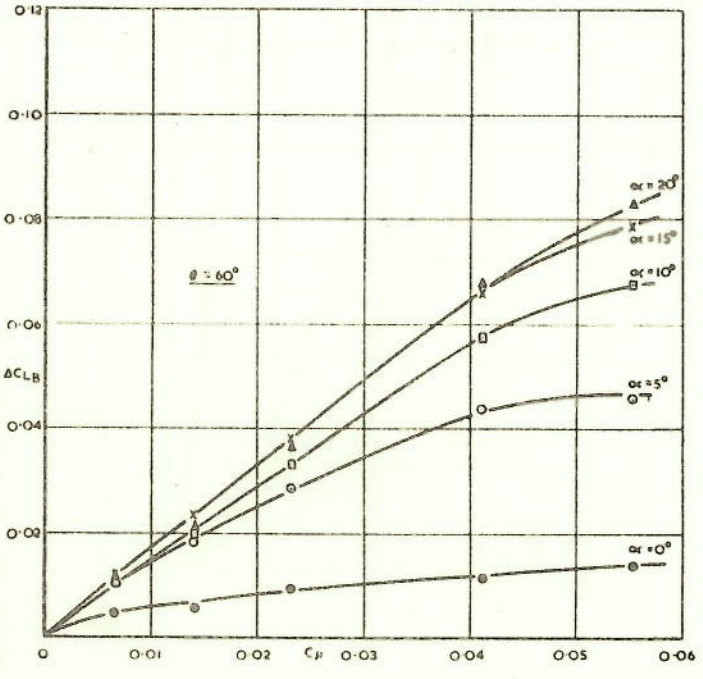

FIG. 18. VARIATION OF LIFT INCREMENT DUE TO BLOWING WITH MOMENTUM COEFFICIENT L.E. BLOWING ONLY. $\phi = 0°$, $\theta = 60°$.

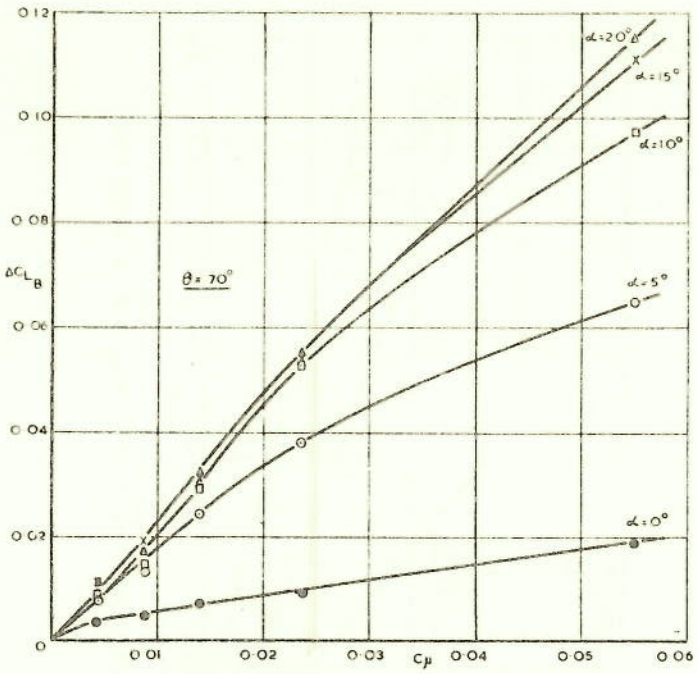

FIG. 19. VARIATION OF LIFT INCREMENT DUE TO BLOWING WITH MOMENTUM COEFICIENT. L.E. BLOWING ONLY. $\phi = 0$, $\theta = 70°$.

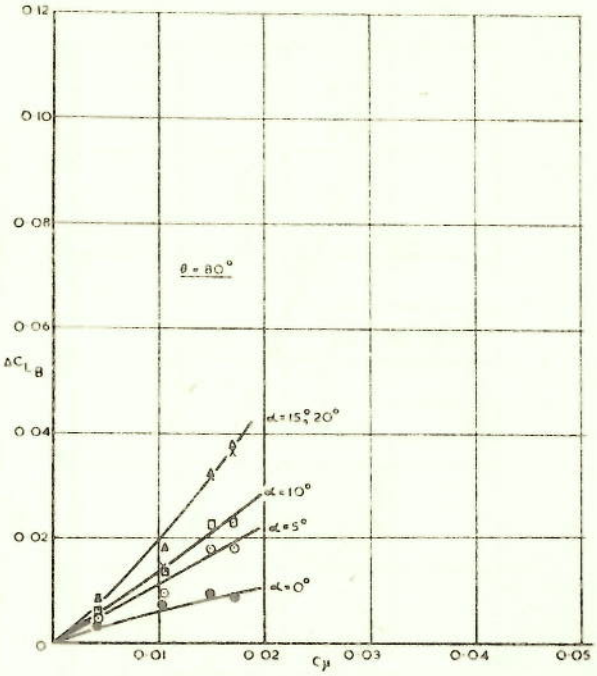

FIG. 21. VARIATION OF LIFT INCREMENT DUE TO BLOWING WITH MOMENTUM COEFICIENT. BLOWING FROM APEX. $\phi = 0$, $\theta = 80°$

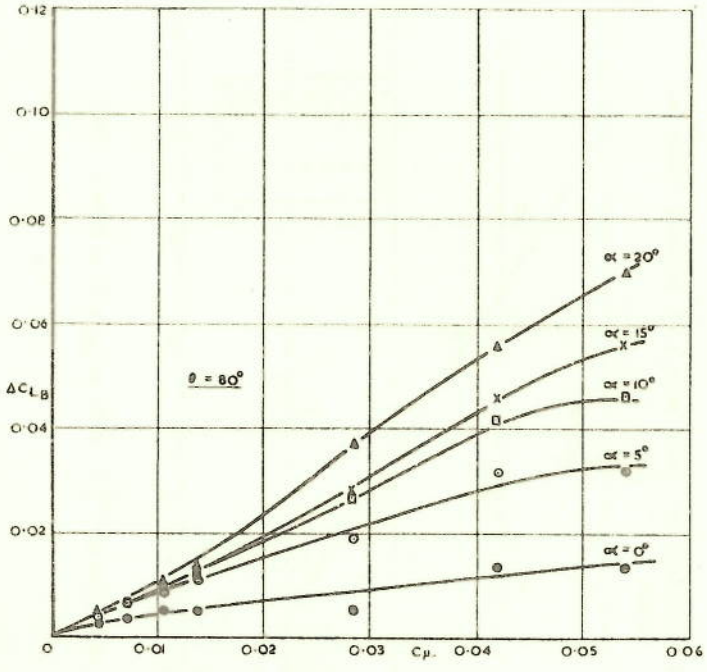

FIG. 20. VARIATION OF LIFT INCREMENT DUE TO BLOWING WITH MOMENTUM COEFFICIENT. L.E. BLOWING ONLY. $\phi = 0°$, $\theta = 80°$

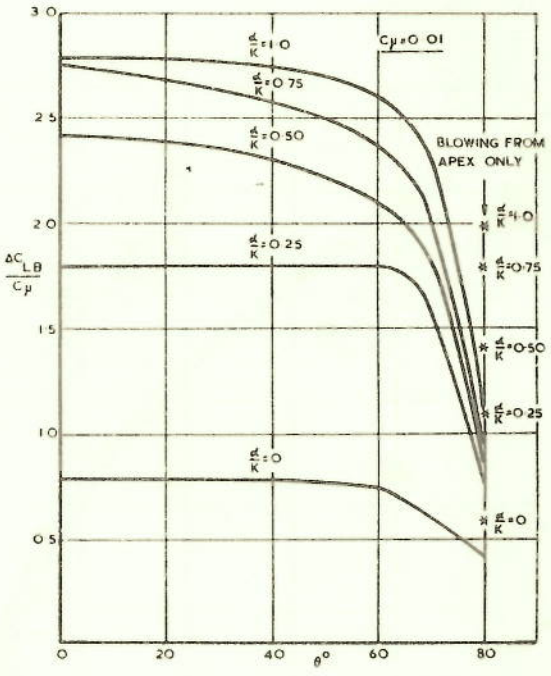

FIG. 22. VARIATION OF LIFT AUGMENTATION $\left(\frac{\Delta C_{LB}}{C_\mu}\right)$ WITH JET SWEEP ANGLE θ.

$\phi = 0$, $C_\mu = 0{\cdot}01$.

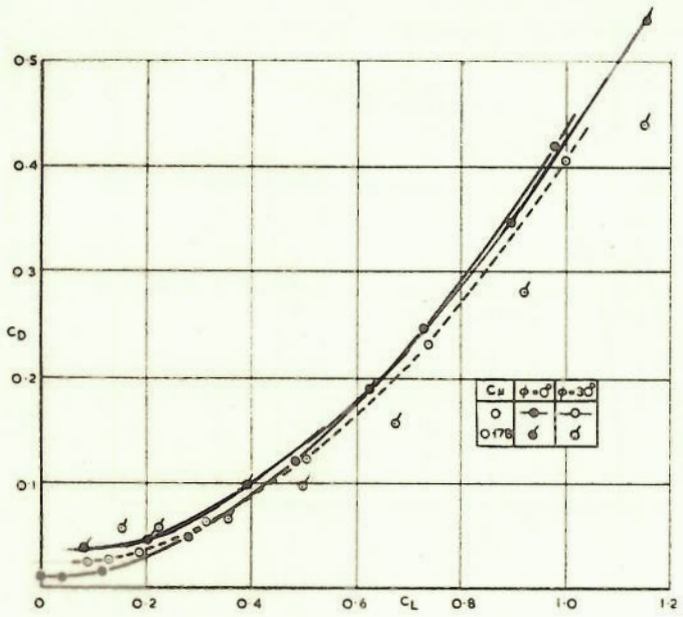

FIG. 23. VARIATION OF DRAG WITH LIFT. BLOWING FROM ALL EDGES.

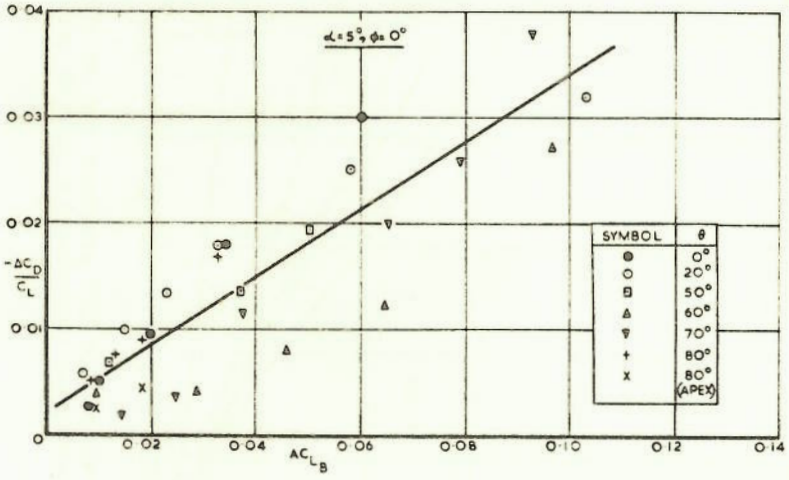

FIG. 24. VARIATION OF $\frac{-\Delta C_D}{C_L}$ WITH ΔC_{L_B} L.E. BLOWING ONLY.

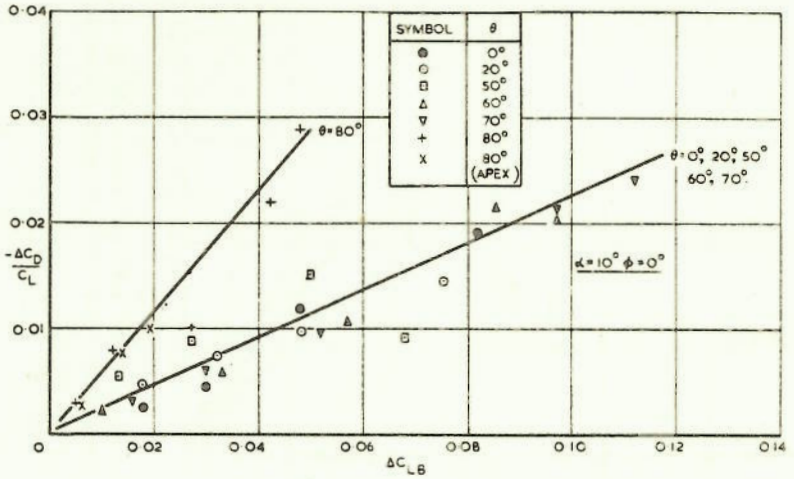

FIG. 25. VARIATION OF $\frac{-\Delta C_D}{C_L}$ WITH ΔC_{L_B} L.E. BLOWING ONLY.

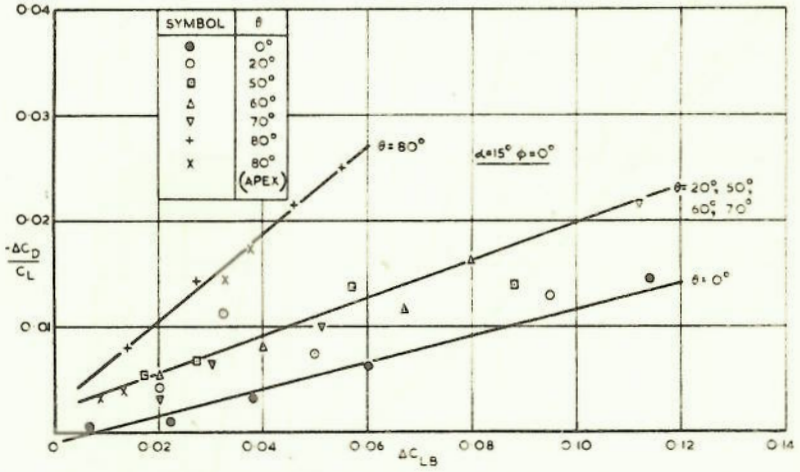

FIG. 26. VARIATION OF $\frac{-\Delta C_D}{C_L}$ WITH ΔC_{L_B} L.E. BLOWING ONLY.

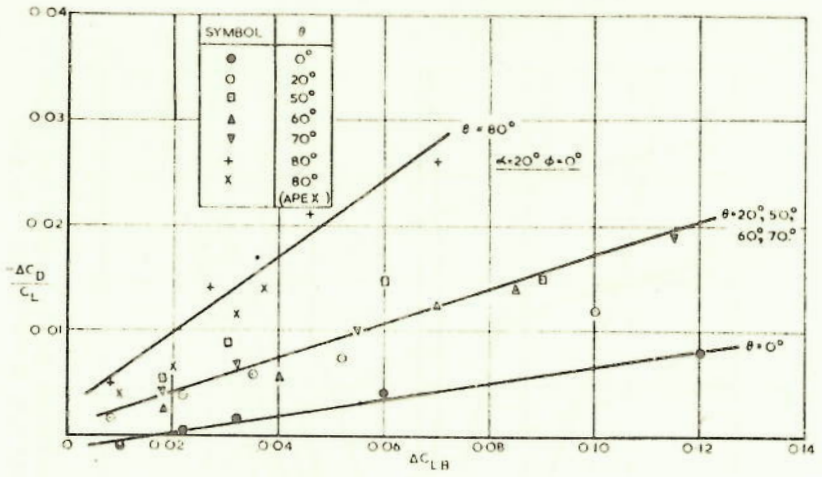

FIG. 27. VARIATION OF $\frac{-\Delta C_D}{C_L}$ WITH ΔC_{LB} L.E. BLOWING ONLY.

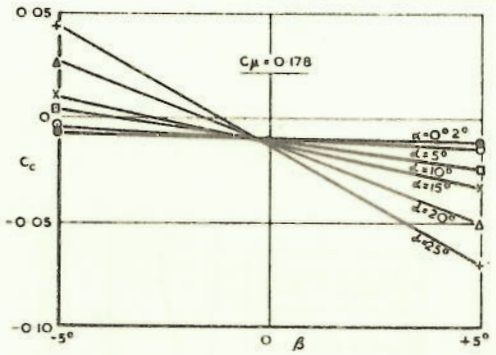

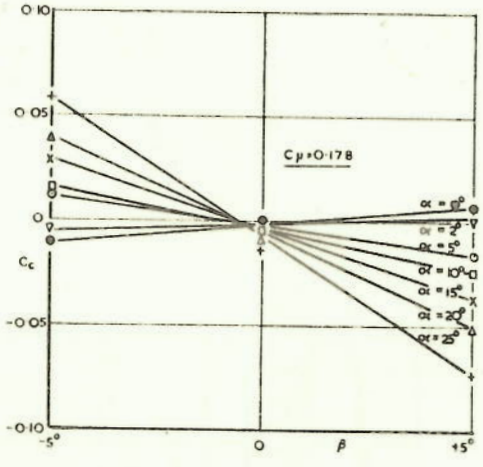

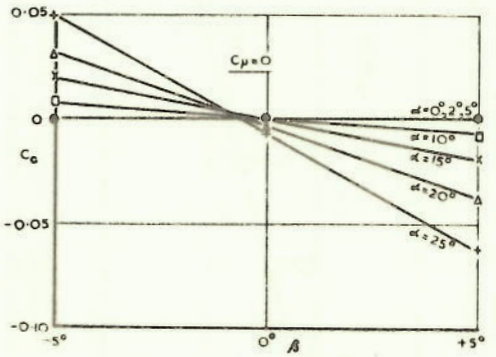

FIG. 28. VARIATION OF CROSS-WIND FORCE WITH SIDESLIP ANGLE β. $\phi = 0°$ BLOWING FROM ALL EDGES.

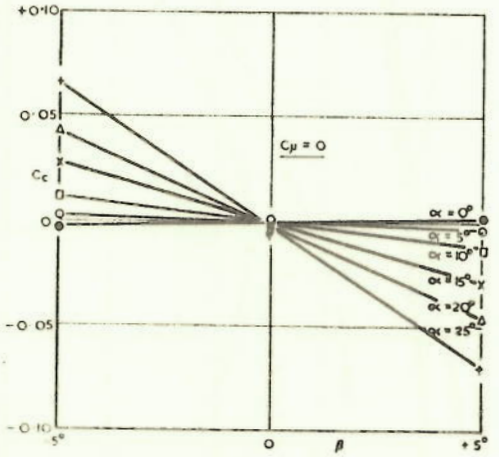

FIG. 29. VARIATION OF CROSS WIND FORCE WITH SIDE SLIP ANGLE β. $\phi = 30°$ BLOWING FROM ALL EDGES.

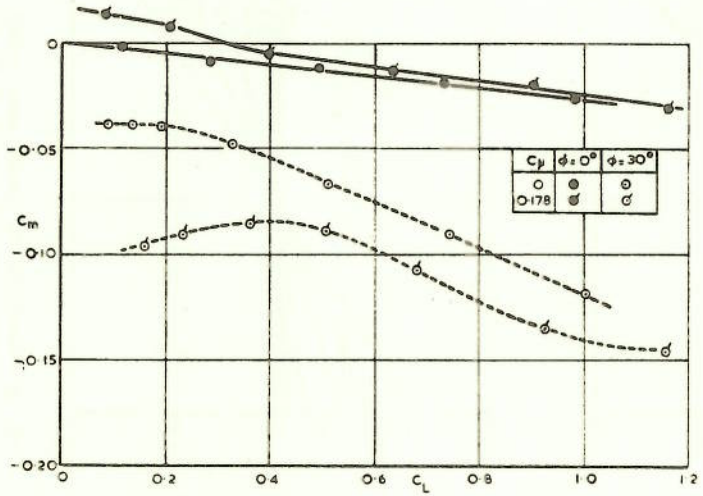

FIG. 30. VARIATION OF PITCHING MOMENT ABOUT MID ROOT CHORD WITH LIFT. BLOWING FROM ALL EDGES.

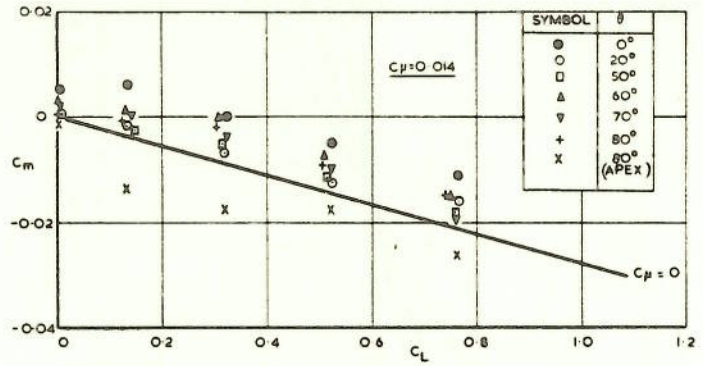

FIG. 32. VARIATION OF PITCHING MOMENT ABOUT MID-CHORD WITH LIFT. L.E. BLOWING ONLY. ϕ = 0.

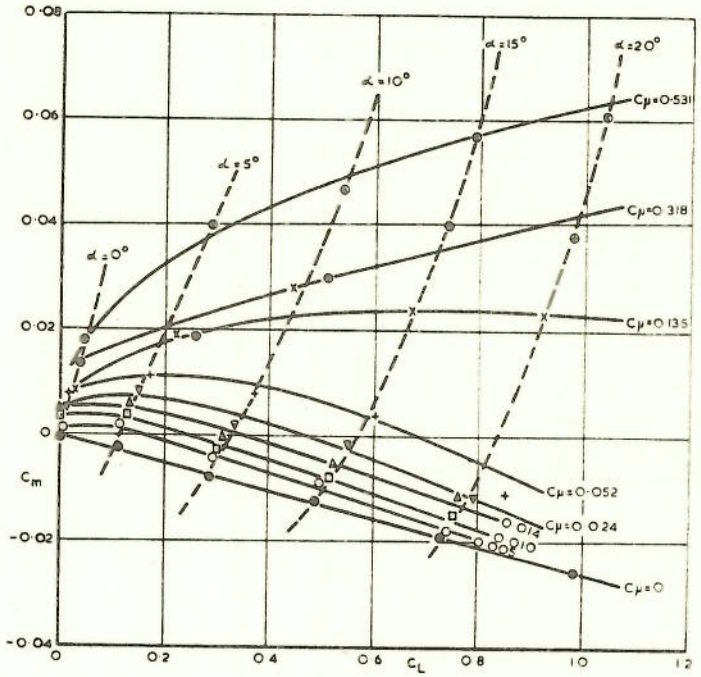

FIG. 31. VARIATION OF PITCHING MOMENT ABOUT MID ROOT CHORD WITH LIFT. L.E. BLOWING ONLY. ϕ = θ = 0.

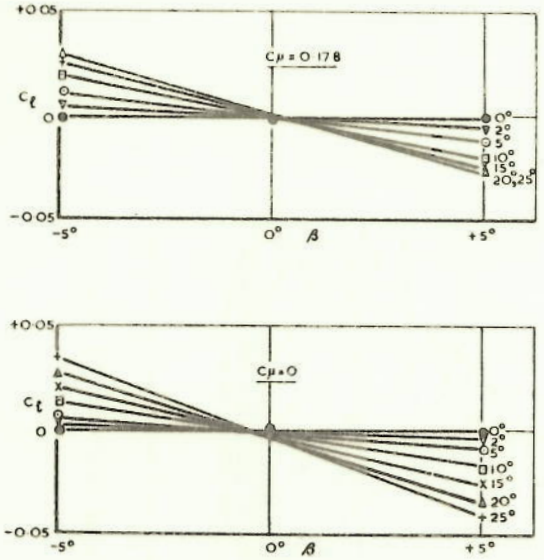

FIG. 33. VARIATION OF ROLLING MOMENT WITH SIDESLIP ANGLE β. BLOWING AT ALL EDGES. $\phi = 0°$.

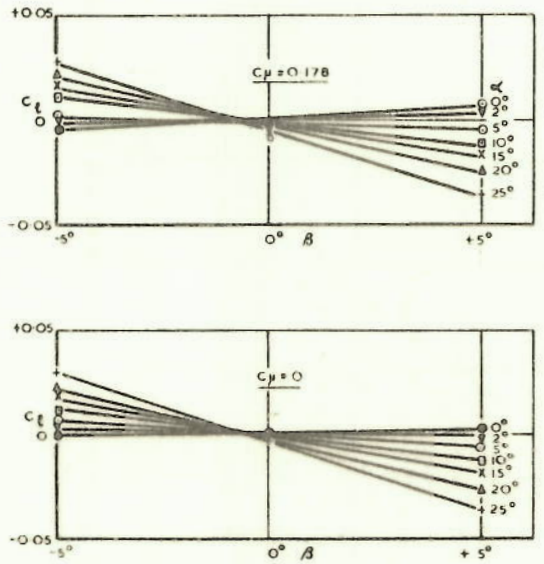

FIG. 34. VARIATION OF ROLLING MOMENT WITH SIDESLIP ANGLE β. BLOWING AT ALL EDGES. $\phi = 30°$.

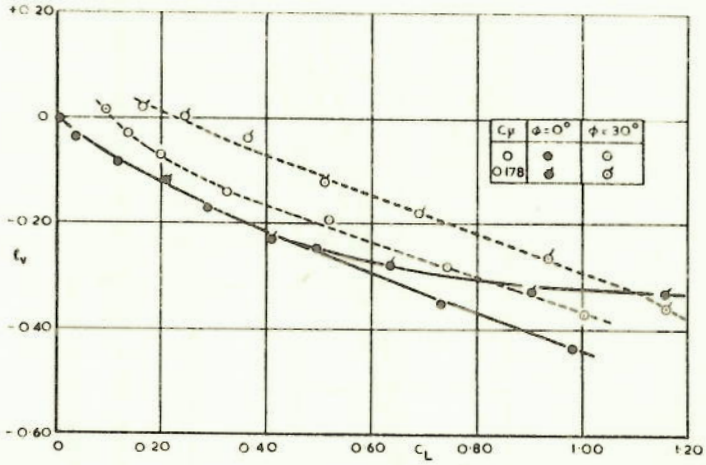

FIG. 35. VARIATION OF $\ell_v \left(\pm\frac{\partial C_\ell}{\partial \beta}\right)$ WITH LIFT. BLOWING FROM ALL EDGES. $\phi = 0°$ & $30°$.

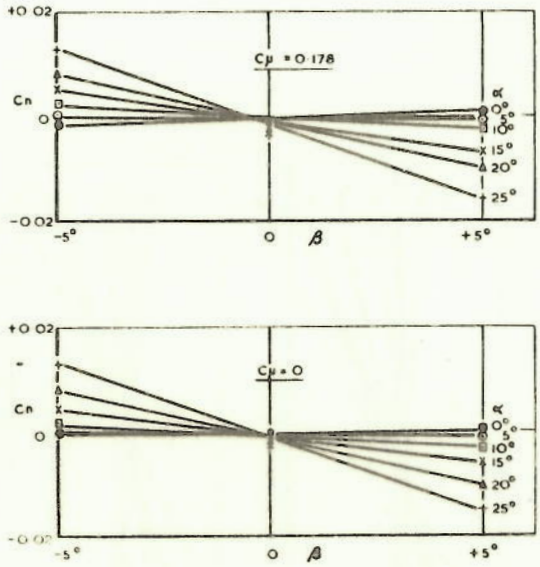

FIG. 36. VARIATION OF YAWING MOMENT WITH SIDESLIP ANGLE β. BLOWING FROM ALL EDGES. $\phi = 0°$.

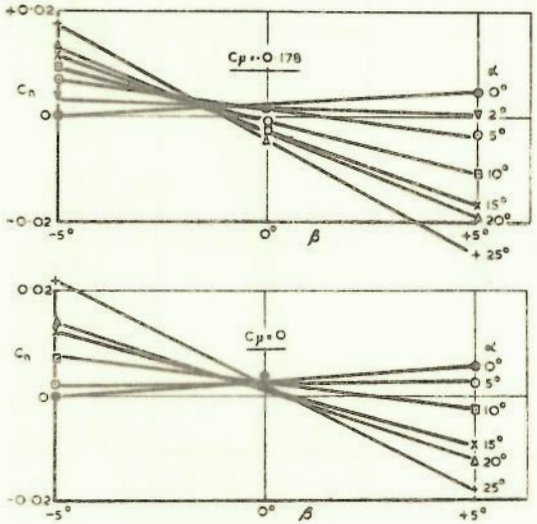

FIG. 37. VARIATION OF YAWING MOMENT WITH SIDESLIP ANGLE β. BLOWING FROM ALL EDGES. $\phi = 30°$.

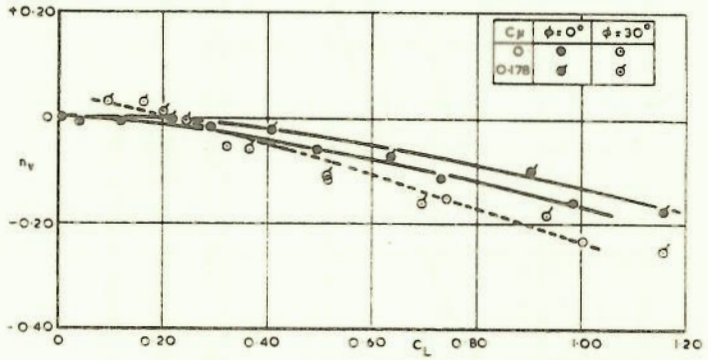

FIG. 38. VARIATION OF $n_v \left(\equiv \frac{\partial C_n}{\partial \beta}\right)$ WITH LIFT. BLOWING FROM ALL EDGES. $\phi = 0°$ & $30°$.

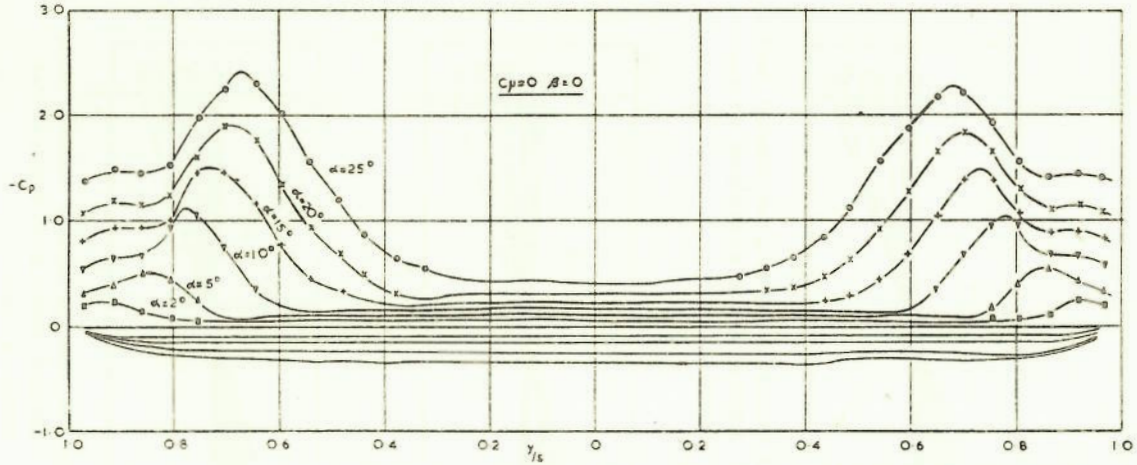

FIG. 39. SPANWISE VARIATION OF UPPER AND LOWER SURFACE STATIC PRESSURE DISTRIBUTIONS. $\infty/c_0 = 0·49$.

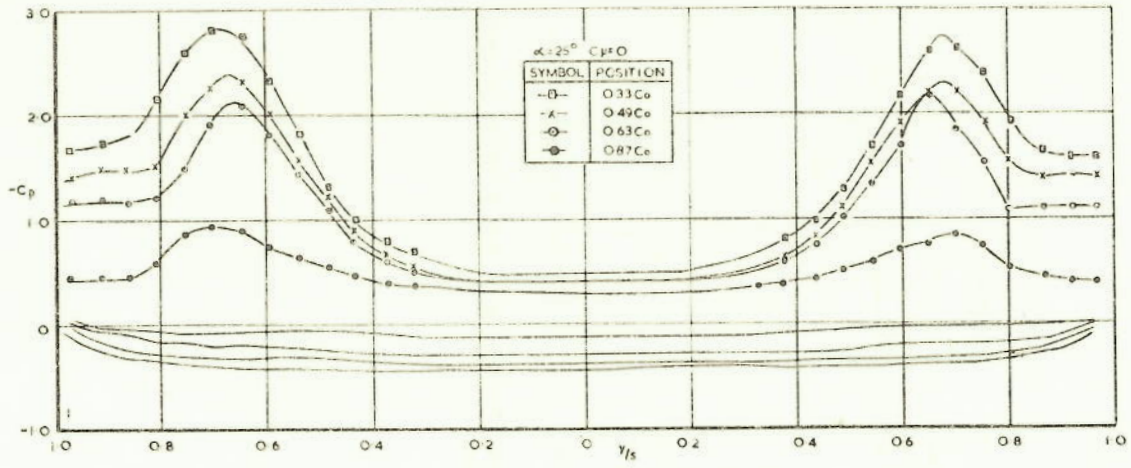

FIG. 40. VARIATION OF SPANWISE STATIC PRESSURE DISTRIBUTIONS WITH α. $\beta = 0$

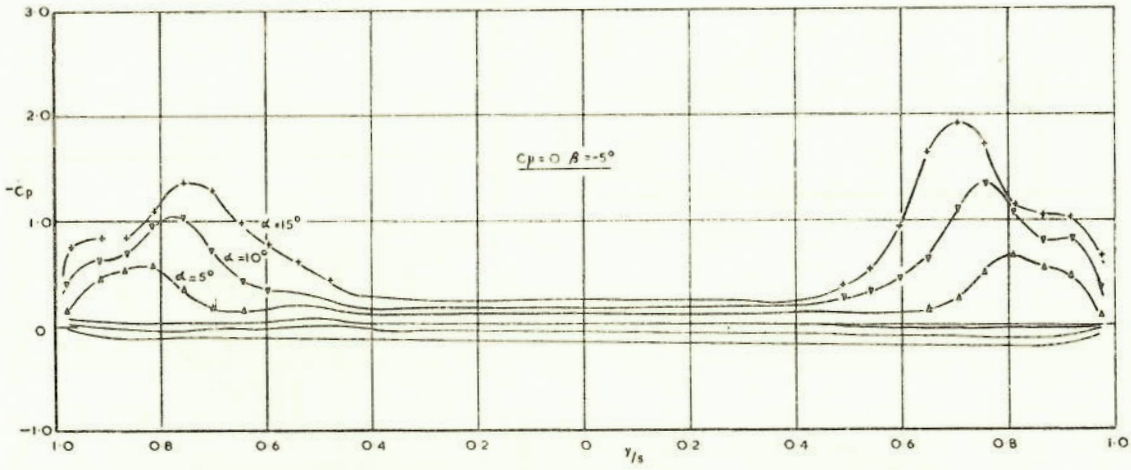

FIG. 41. SPANWISE VARIATION OF UPPER AND LOWER SURFACE STATIC PRESSURE DISTRIBUTIONS. $x/c_o = 0{\cdot}49$.

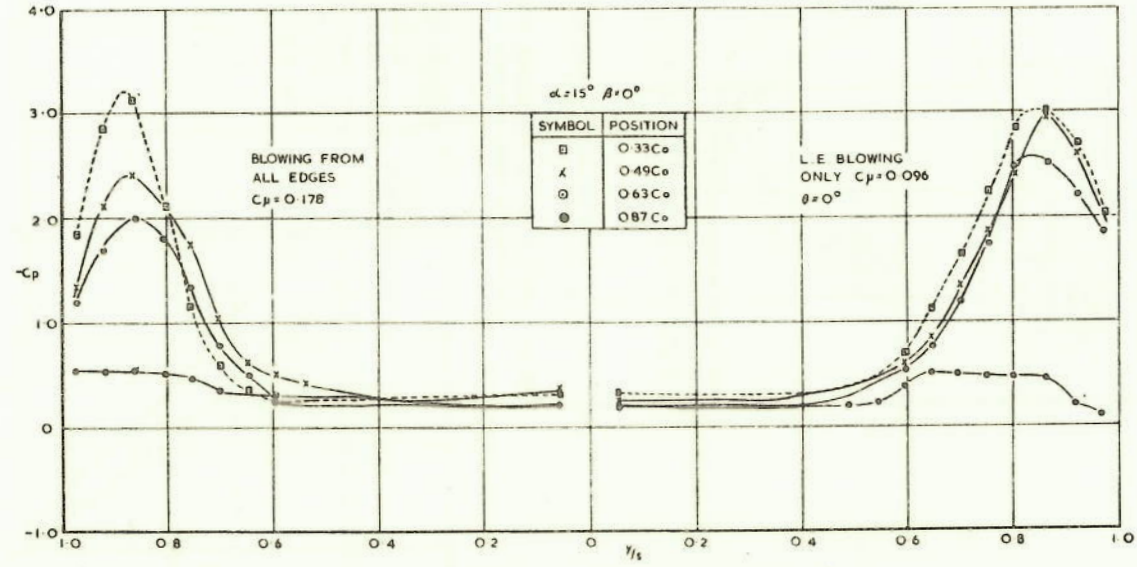

FIG. 42. CHORDWISE VARIATION OF UPPER SURFACE SPANWISE STATIC PRESSURE DISTRIBUTIONS WITH BLOWING.

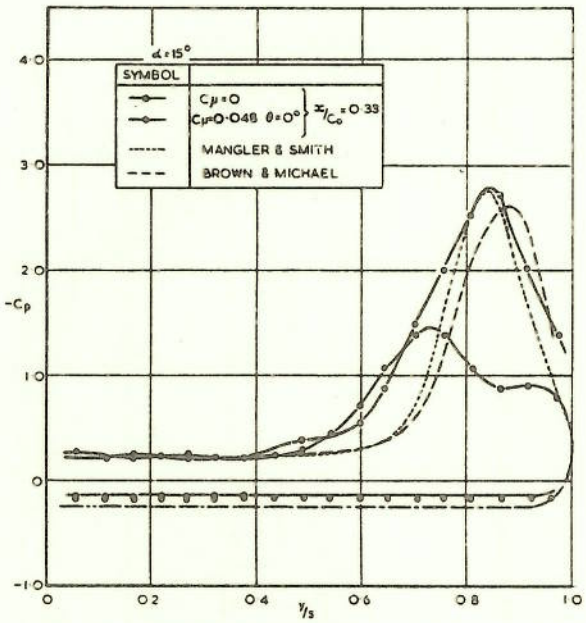

FIG. 43. SURFACE STATIC PRESSURE DISTRIBUTIONS. COMPARISON WITH THEORY.

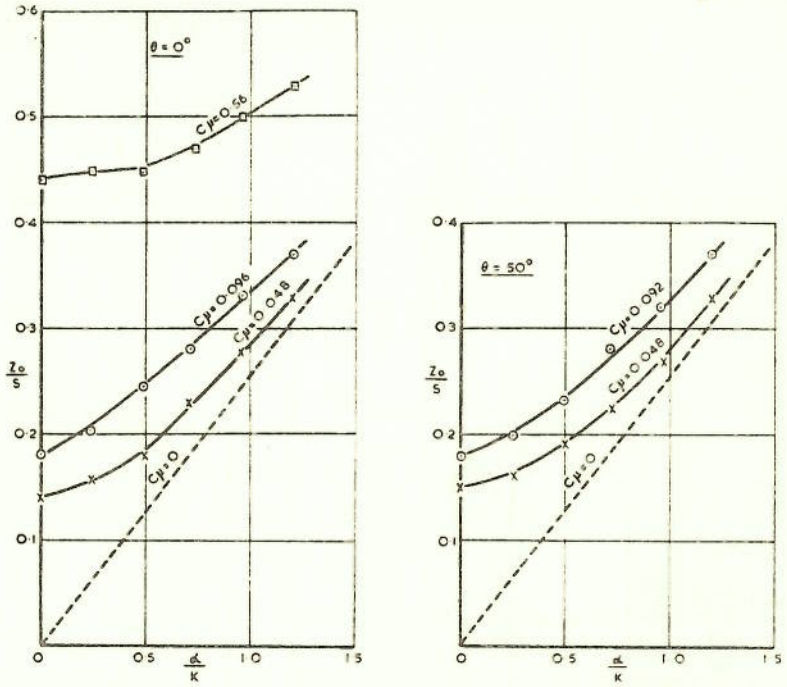

FIG. 45a & 45b. VORTEX CORE POSITIONS WITH AND WITHOUT LEADING EDGE BLOWING.

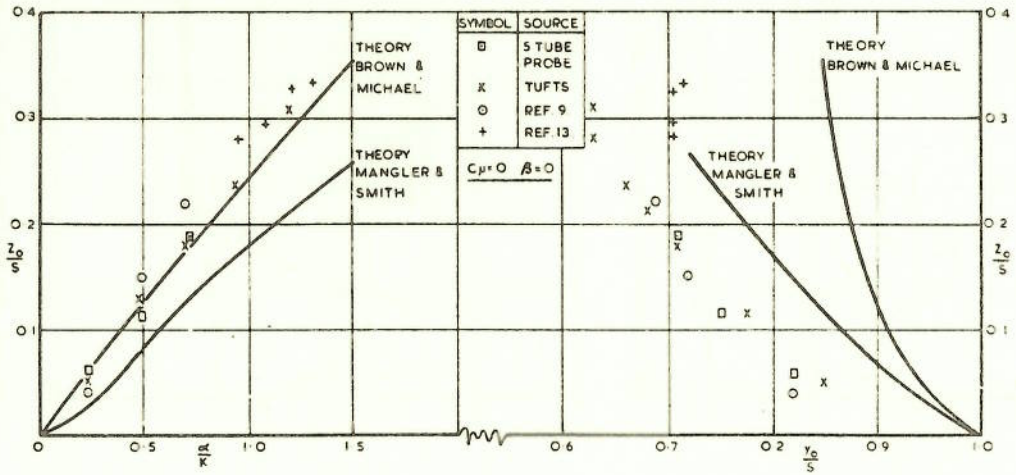

FIG. 44. VORTEX CORE POSITIONS FOR Cμ = 0. COMPARISON WITH THEORY.

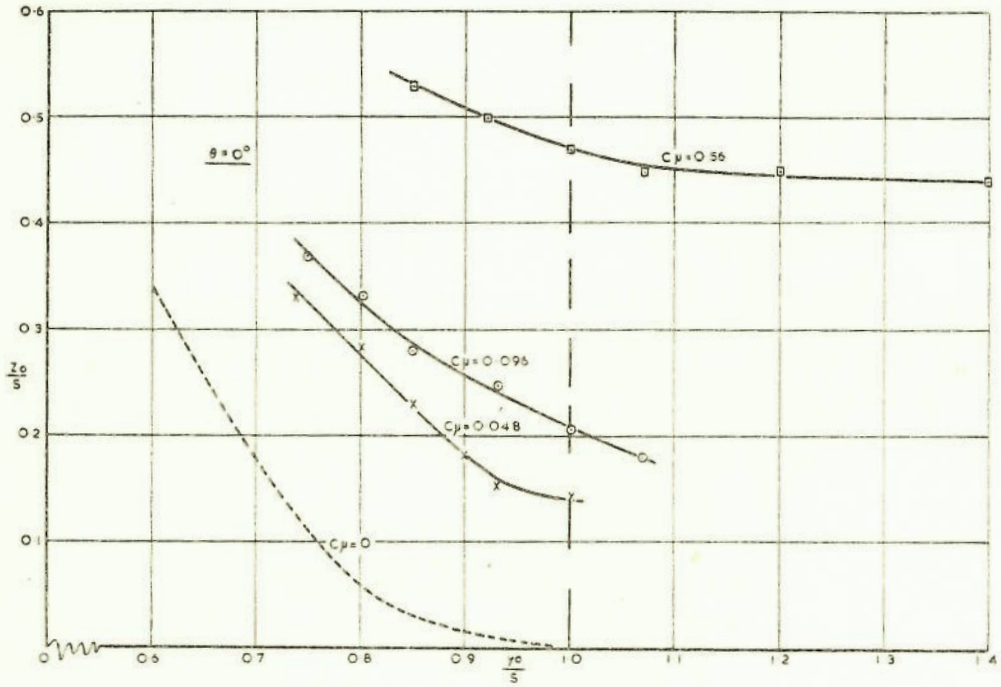

FIG. 46a. VORTEX CORE POSITIONS, WITH AND WITHOUT LEADING EDGE BLOWING.

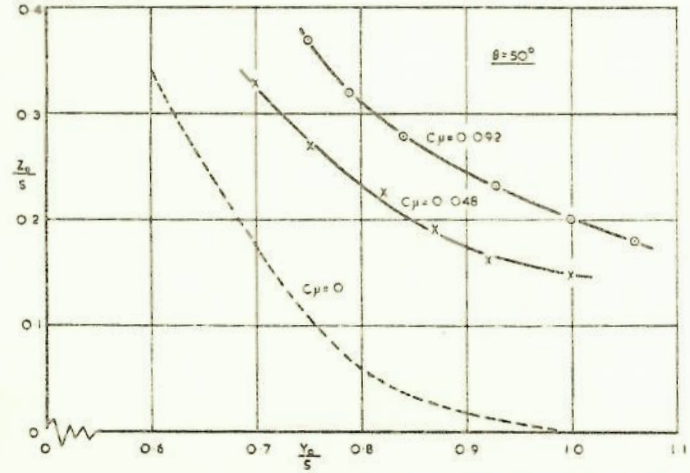

FIG. 46b. VORTEX CORE POSITIONS WITH AND WITHOUT LEADING EDGE BLOWING.

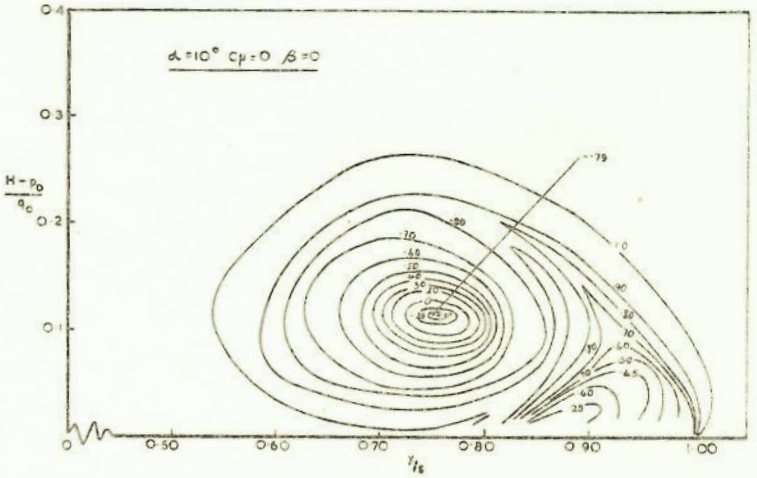

FIG. 47. VARIATION OF TOTAL HEAD THROUGH VORTEX. $C\mu = 0$, $x/c_0 = 0.50$.

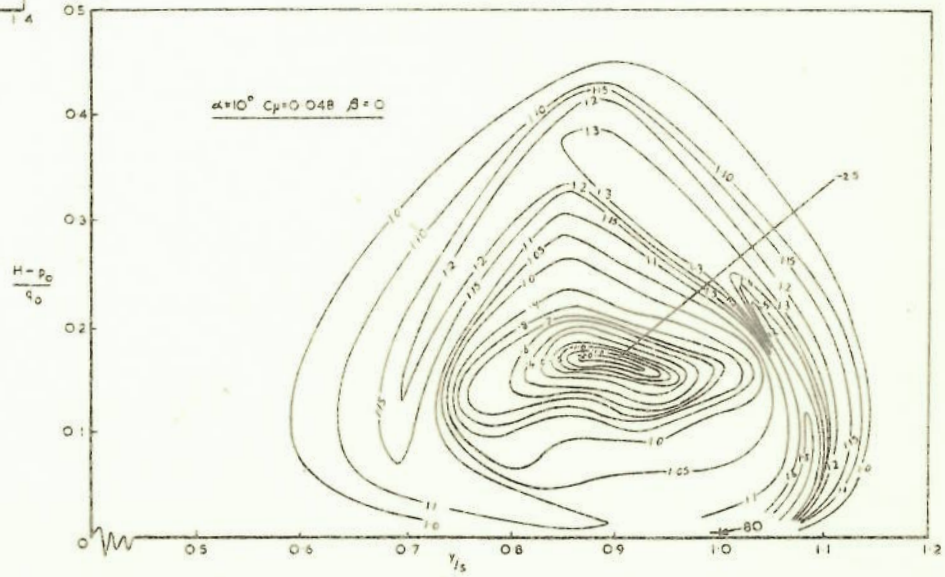

FIG. 48. VARIATION OF TOTAL HEAD THROUGH VORTEX. $C\mu = 0.048$, $x/c_0 = 0.50$. $\theta = 0°$.